2008

EMPIRICAL AND NUMERICAL SITE-RESPONSE CALCULATIONS AT POLARIS SEISMOGRAPH STATIONS

Kimberly Read

EMPIRICAL AND NUMERICAL SITE-RESPONSE CALCULATIONS AT POLARIS SEISMOGRAPH STATIONS

SPINE TITLE: SITE RESPONSE CALCULATIONS AT POLARIS SEISMOGRAPH STATIONS

(Thesis format: Integrated-Article)

By

Kimberly Read

Faculty of Engineering
Department of Civil and Environmental Engineering

Submitted in partial fulfillment
of the requirements for the degree of
Master of Engineering Science

School of Graduate and Postdoctoral Studies
The University of Western Ontario
London, Ontario, Canada
December, 2008

ABSTRACT

Determining ground motion amplification resulting from a site's near-surface layers is important to earthquake hazard assessment. Site-response spectra may be used to quantify this response using either empirical or numerical methods.

In this thesis, site-response spectra were determined for eleven POLARIS sites using two popular empirical methods: Nakamura's microtremor method and the horizontal-to-vertical spectral ratio (HVSR) method. A correlation between the type of the near-surface conditions (soil or rock) and the spectral shape was observed. While hard rock sites exhibited frequency-independent amplification ranging from near unity at 1 Hz, to 2 at 5 Hz, soil sites were characterized by a resonant peak at the fundamental frequency (f_0). Both methods predicted similar values of f_0 at each of the soil sites. Seismic refraction surveys were conducted at the soil stations, and used to produce numerical spectra which validated those produced empirically.

Further, numerical site-response modelling was conducted using three programs: EERA, NERA and QUAKE/W, at five POLARIS soil sites, for earthquakes of varying intensity levels. For earthquakes of low and moderate intensity, all programs agreed well. At higher intensity levels, results from the equivalent-linear programs were inconsistent with those produced using nonlinear analysis.

Keywords: *amplification, site-response, POLARIS, EERA, NERA, QUAKE/W.*

ACKNOWLEDGEMENTS

I would like to express my appreciation to my supervisor, Dr. Hesham El Naggar, for the guidance he provided during my graduate school experience. To my supervisory committee member, Dr. David Eaton, I would also like to extend my sincere gratitude for all of his advice and assistance, which made much of this thesis possible.

I would also like to thank Savka Dineva, for her help with numerous aspects of this project. Her knowledge of the POLARIS network and her assistance, both at school and in the field, proved invaluable.

Many thanks to Wayne Edwards, for providing the refraction data collected at Elginfield, and for his kind help with the related MATLAB code.

Thanks to Dimitry Mihaylov, Kadircan Aktas, and Catrina Alaksandrakis, for their assistance with field work during this study. Their help with procuring equipment and performing the surveys is greatly appreciated.

A great deal of thanks is owed to my mother and father, and my sisters, Gill and Kelly, for all their encouragement, love and patience during this process. Finally, thank you to Morgan Bickerdike, for all the understanding and support he has provided.

TABLE OF CONTENTS

LIST OF TABLES

LIST OF FIGURES

LIST OF SYMBOLS

$a(t)$, $A(f)$	wave amplitude
$e(t)$, $E(f)$	source effects
f_0	fundamental frequency
G	shear modulus
h	thickness
$H(f)$	horizontal spectrum
$i(t)$, $I(f)$	instrument response
M	earthquake magnitude
$\overline{N}$	average standard penetration resistance
PI	plasticity index
$p(t)$, $P(f)$	path effects
R	hypocentral distance
R_y	ratio of effective shear strain
$s(t)$, $S(f)$	local site effects
$\overline{S_u}$	average undrained shear strength
$V(f)$	vertical spectrum
v, V_s	shear-wave velocity
$\overline{V_{30}}$	average shear-wave velocity in the top 30 m of the site
w	moisture content
x_c	critical distance
γ_{eff}	effective shear strain

γ_{max}	maximum shear strain
γ_s	soil unit weight
ξ	damping ratio
ρ	density

CHAPTER 1

INTRODUCTION

1.1 GENERAL

The influence of local site conditions on the characteristics of earthquake ground motion is widely recognized among seismologists and geotechnical engineers (Bardet et al. 2001). Such local site effects are evidenced by the uneven damage distribution from numerous historical earthquakes, where high levels of structural damage can be correlated with sites that have soils, as opposed to rock, near the surface (e.g. MacMurdo 1824). Damage patterns from more recent earthquakes, including the 1985 Michoacan earthquake (e.g. Singh et al. 1988), the 1989 Loma Prieta earthquake (e.g. Borcherdt and Glassmoyer 1992), the 1994 Northridge earthquake (e.g. Hartzell et al. 1996), and the 1999 Izmit earthquake (e.g. Özel et al. 1999) further illustrate the role site effects play in contributing to earthquake damage. Observations from these studies indicate that, generally, soft soils tend to amplify ground motion in comparison to more competent soils and bedrock. Given the potentially destructive nature of this amplification, precise knowledge of local site response becomes important, particularly in areas where critical structures are located (Field and Jacob 1995). As a result, the development and testing of methods which can quantify site response has become a fertile area of research.

Site-response studies typically define the localized amplification using site-response spectra, frequency-dependent functions representing the response at a given soil site relative to the response that would be experienced by a competent bedrock site for the same earthquake (Presti et al. 2006). Current approaches for determining these

spectra primarily fall into two broad categories: empirical or theoretical (Lermo and Chavez-Garcia 1994). Empirical approaches rely on observed measurements of ground motion, while theoretical methods attempt to evaluate site response analytically using the dynamic properties of the site's near-surface soils. The purpose of this thesis is to investigate some of the methods that can be used to estimate site response, with the ultimate goal of providing some technical guidance about their validity and suitability for assessing local site effects.

1.2 BACKGROUND

As part of this study, data related to several sites in the POLARIS (Portable Observatories for Lithospheric Analysis Investigating Seismicity) network were used to examine various empirical and theoretical approaches to site-response evaluation. The POLARIS network consists of geophysical observatories located in Ontario, British Columbia, the Northwest Territories, Quebec, Nunavut and Nova Scotia (Figure 1.1). These observatories provide live data for research, education, and the continuous monitoring of earthquakes (www.polarisnet.ca).

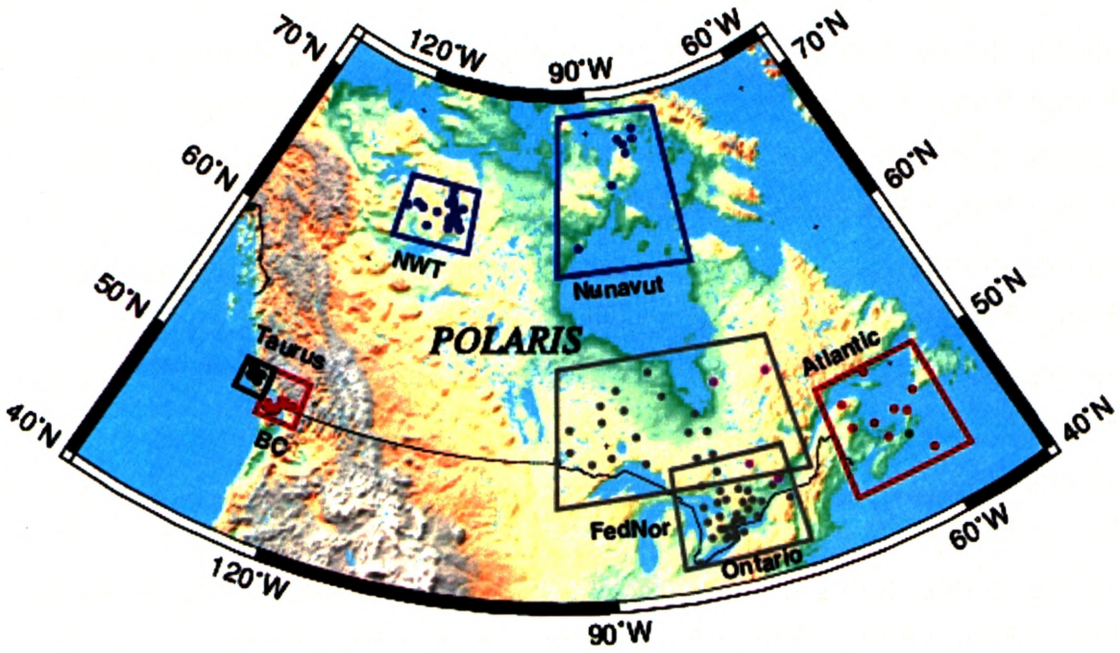

Figure 1.1: Canadian POLARIS arrays (www.polonet.ca).

The Ontario array of POLARIS stations (the POLO array) covers a roughly rectangular area within the lower Great Lakes region (see Figure 1.2) (Murphy and Eaton 2005). Some POLO stations, particularly those in the eastern part of the array, rest on competent Precambrian bedrock (Murphy 2003). This bedrock provides an ideal foundation for such stations; however, much of southern Ontario lacks bedrock exposures (Beresnev and Atkinson 1997). As a consequence, many of the seismograph stations in the POLO array are located on thick overburden or weathered Paleozoic limestone (Murphy and Eaton 2005).

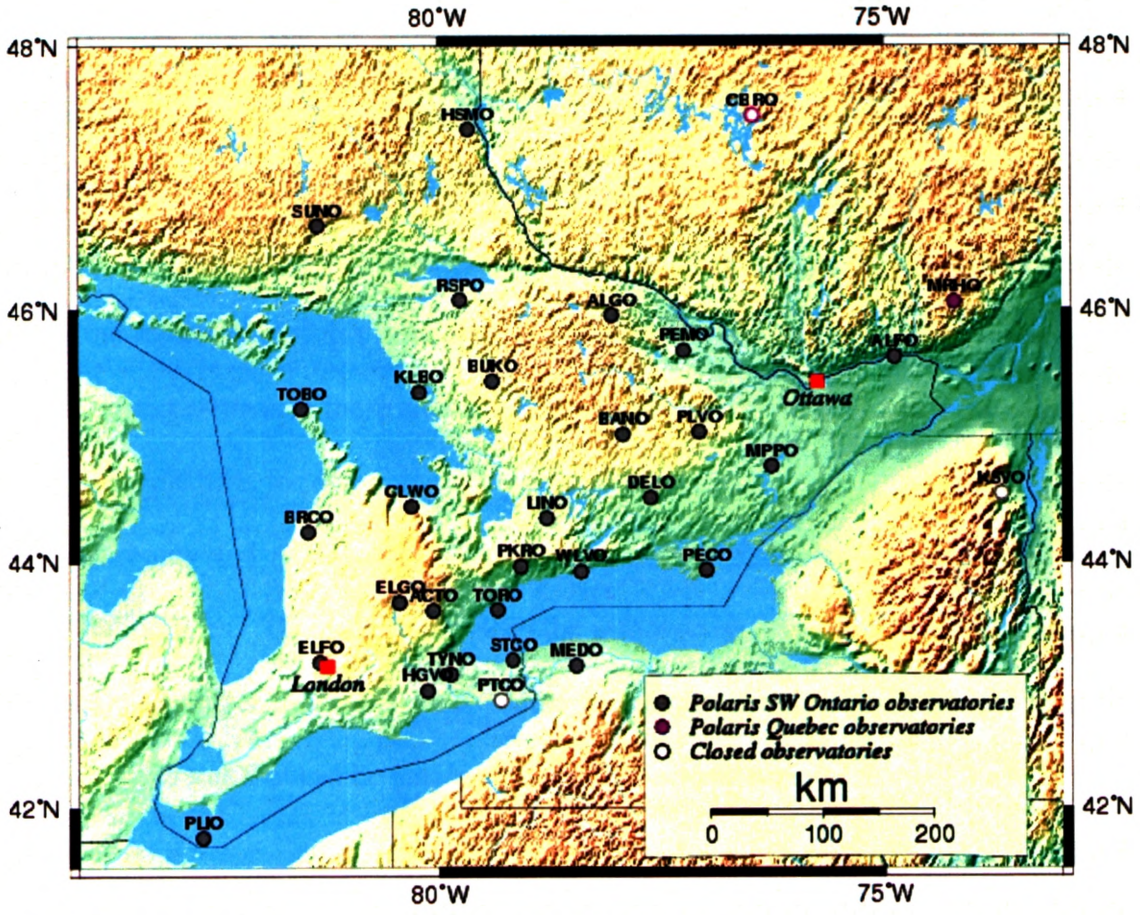

Figure 1.2: Southern Ontario POLARIS stations in 2004 (www.polonet.ca).

The variable near-surface conditions at the POLO sites present a problem when comparing seismograms of regional and teleseismic (i.e. >1000 km from the site) events recorded at different stations. Use of these recordings for research pursuits, including earthquake magnitude calculation, is possible only if the local ground response at each station can be properly quantified. The geographical coverage of this network will potentially improve magnitude estimates; therefore, producing a quantitative means of removing the effects of local site amplification from the waveforms would be advantageous (Murphy 2003).

To this end, Murphy and Eaton (2005) produced site-response spectra for the eighteen POLO stations that were operational at the time of their study. The subsequent expansion of the POLO network involved adding new stations whose site response was unknown. Determination of site-response spectra at these sites is, therefore, necessary to further the calibration of this network. In addition, the availability of data collected by the monitoring stations at these sites provides an opportunity to evaluate the applicability of empirical methods for determining site-response spectra.

Beresnev and Atkinson (1997) produced near-surface profiles for several of the POLO station sites. Their study provides the information necessary to create numerical models for a number of POLO sites. Some of these profiles are used here to examine computer programs that can be employed for theoretical site-response modelling.

1.3 OBJECTIVES

This investigation examines various methods that are commonly used for evaluating local site effects with the following specific objectives:

1. To advance the calibration of the POLO network by providing empirically-produced site-response spectra for eleven POLO stations.
2. To compare and validate two popular empirical approaches used to generate site-response spectra, namely Nakamura's (1989) microtremor analysis method, and the horizontal-to-vertical spectra ratio (HVSR) method of Lermo and Chavez-Garcia (1993).
3. To examine the suitability of three modelling programs for predicting site response at various levels of ground shaking: the Equivalent-linear Earthquake

Response Analysis (EERA) program of Bardet et al. (2000), the finite-element modelling program QUAKE/W 2004 (Krahn 2004), and the Nonlinear Earthquake site Response Analysis (NERA) program of Bardet and Tobita (2001).

1.4 THESIS STRUCTURE

This thesis is organized into five chapters, which address the objectives presented above.

Chapter 2 provides the necessary theoretical background, and a review of related previous studies.

Chapter 3 presents a study of the two empirical methods for site-effect evaluation. Using these methods, site-response spectra are produced for eleven POLO stations. Spectra from the two methods are compared. In some cases, simple numerical models are used to assess the validity of these empirical spectra.

Numerical computation of site-response spectra is investigated in Chapter 4. Theoretical spectra are produced using three modelling programs for five POLO stations, and the results are compared.

The thesis concludes with Chapter 5, which provides a summary and discussion of the entire study.

REFERENCES

Bardet, J. P., Ichii, K., and Lin, C. H. (2000). *EERA: A Computer Program for Equivalent Linear Earthquake Site Response Analysis of Layered Soil Deposits*, University of Southern California, Department of Civil Engineering.

Bardet, J. P., and Tobita, T. (2001). *NERA: A Computer Program for Nonlinear Earthquake site Response Analyses of Layered Soil Deposits*, University of Southern California, Department of Civil Engineering.

Bardet, J. P., Tobita, T., Ichii, K., and Rogers, A. (2001). "Site response analysis at the vertical arrays of the Cerritos College Police Station and San Bernadino Main Fire Station." *A report to the USGS on Collaborative Research between GeoRisk Associates, Inc. and the University of Southern California*, University of Southern California, Department of Civil Engineering.

Beresnev, I., and Atkinson, G. M. (1997). "Shear wave velocity survey of seismographic sites in eastern Canada: calibration of empirical regression method of estimating site-response." *Seismological Research Letters*, 68(6), 981-987.

Borcherdt, R. D., and Glassmoyer, G. (1992). "On the characteristics of local geology and their influence on ground motions generated by the Loma Prieta earthquake in the San Francisco Bay region, California." *Bulletin of the Seismological Society of America*, 82(2), 603-641.

Field, E. H. and Jacob, K. H. (1995). "A comparison and test of various site-response estimation techniques, including three that are not reference-site dependent." *Bulletin of the Seismological Society of America*, 85(4), 1127-1143.

Hartzell, S., Leeds, A., Frankel, A., and Michael, J. (1996). "Site response for urban Los Angeles using aftershocks of the Northridge earthquake." *Bulletin of the Seismological Society of America*, 86(1B), S168-S192.

Krahn, J. (2004). *Dynamic Modelling with QUAKE/W: An Engineering Methodology,* GEO-SLOPE International Ltd., Calgary.

Lermo, J. F. and Chavez-Garcia, F. J. (1993). "Site effect evaluation using spectral ratios with only one station." *Bulletin of the Seismological Society of America*, 83(5), 1574-1594.

Lermo, J. F., and Chavez-Garcia, F. J. (1994). "Are microtremors useful in site-response evaluation?" *Bulletin of the Seismological Society of America*, 84(5), 1350-1364.

MacMurdo, J. (1824). "Papers relating to the earthquake which occurred in India in 1819." *Philosophical Magazine*, 63, 105-177.

Murphy, C. (2003). "Near-surface characterization and estimated site response at POLARIS seismograph stations in southern Ontario, Canada." MSc thesis, University of Western Ontario, London, Ontario, Canada.

Murphy, C. and Eaton, D. (2005). "Empirical site response for POLARIS stations in Southern Ontario, Canada." *Seismological Research Letters*, 76(1), 99-109.

Nakamura, Y. (1989). "A method for dynamic characteristics estimation of subsurface using microtremor on the ground surface." *Quarterly Report of the Railway Technical Research Institute*, 30(1), 25-33.

Özel, O., Cranswick, E., Meremonte, M., Erdik, M., and Safak, E. (1999). "Site effects in Avcilar, west of Istanbul, Turkey, from strong- and weak-motion data." *Bulletin of the Seismological Society of America*, 92(1), 499-508.

Presti, D. C. F. L., Lai, C. G., and Puci, I. (2006). "ONDA: Computer code for nonlinear seismic response analyses of soil deposits." *Journal of Geotechnical and Geoenvironmental Engineering,* 132(2), 223-236.

Singh, S. K., Lermo, J., Dominguez, T., Ordaz, M., Espinosa, J. M., Mena, E., and Quass, R. (1988). "The Mexico earthquake of September 19, 1985 - a study of amplification of seismic waves in the valley of Mexico with respect to a hill zone site." *Earthquake Spectra*, 4(4), 653-673.

CHAPTER 2

LITERATURE REVIEW

2.1 INTRODUCTION

During an earthquake, accumulated strain energy is released from a focal region and propagates through the surrounding earth. The characteristics of an earthquake observed at a given point on the surface are, therefore, influenced by three factors: the radiation characteristics of the source; the kinematic and dynamic characteristics of the route from source to observation point; and the kinematic and dynamic characteristics of the near-surface layers at the observation point (Nakamura 1989). In the time domain, the observed motion at a given site (a) may be written in terms of the earthquake source (e), path (p), and local site effects (s), and the response of the recording instrument (i):

$$a(t) = e(t) * p(t) * s(t) * i(t) \tag{2.1}$$

where * denotes convolution (Kramer 1996). Although all these factors influence the observed waveform, the greatest impact is generally related to local site effects, that is, the response of the uppermost layers of rock and soil at the site (Nakamura 1989).

An example of the impact of local site effects on observed ground response is provided in Figure 2.1, which contains seismograms recorded at four stations during the August 17, 1999, Izmit earthquake. The recording stations have differing near-surface characteristics. Three of the stations (ATS, CNA and DHM) are located on soft soil, while the fourth station (YKP) is located on hard rock. Although the sites have similar source and path effects, differences in the frequency content and amplitudes of the seismograms are notable. More specifically, amplitudes measured at the soil sites are

significantly higher than those measured at the hard-rock site. Such variations can be attributed to the differing near-surface site conditions (Özel et al. 2002).

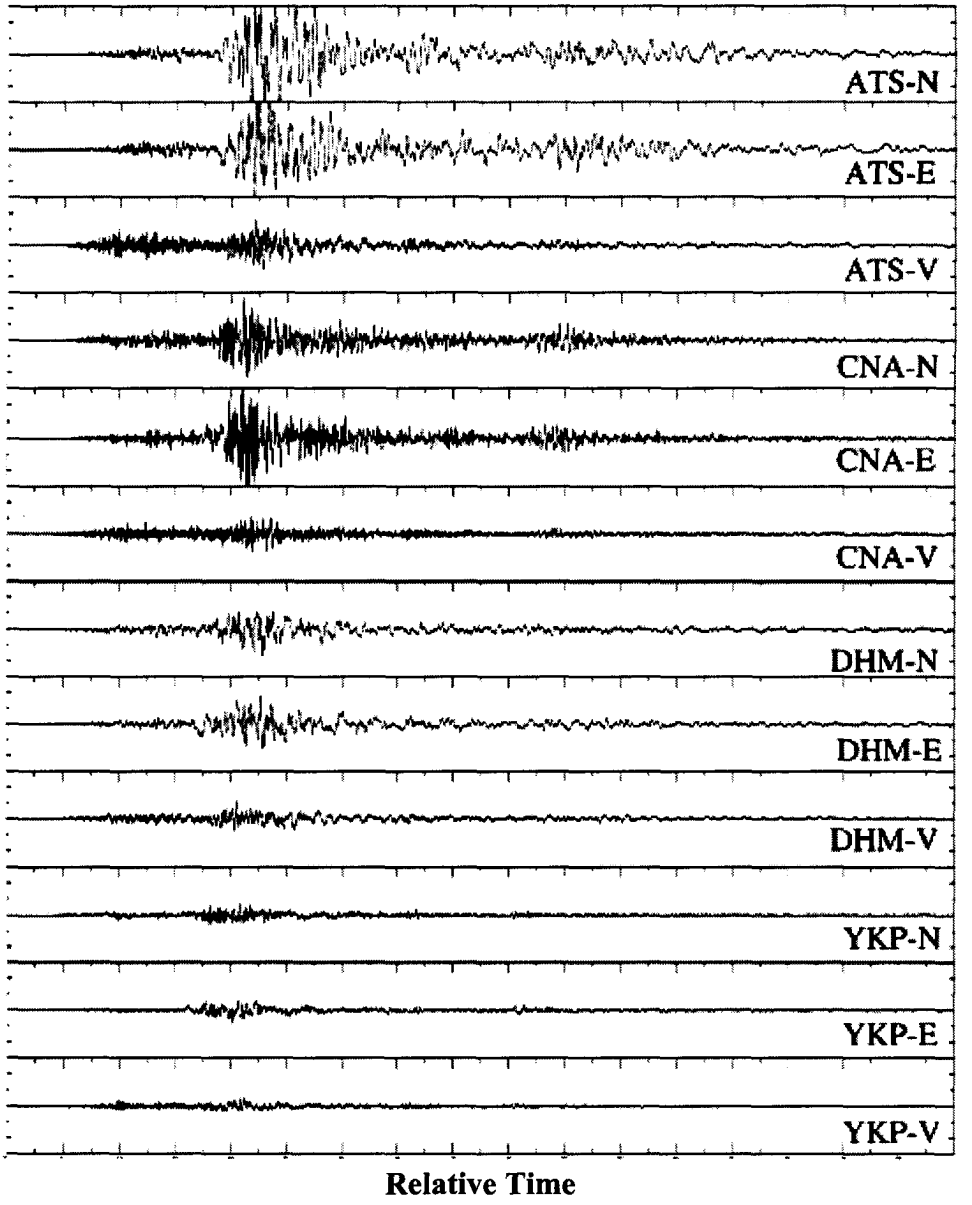

Figure 2.1: Three-component seismograms recorded during the August 17, 1999 Izmit earthquake. Seismograms are equi-scaled from -200 to 200 mg (Özel et al. 2002).

2.1.1 Seismic Waves

Fundamental to discussion of local site effects is an understanding of seismic wave types. Earthquake-produced waves can be divided into two basic categories: body waves, which propagate through the earth's interior; and surface waves, which travel along the earth's surface layers. Body waves are subdivided into primary (compressional) and secondary (shear) waves, know as *P*- and *S*-waves, respectively. For *S*-waves, particle movement, which is perpendicular to the direction of wave travel, can be either horizontal (*SH*-waves) or vertical (*SV*-waves). Surface waves include two important wave systems that can be significant during an earthquake event: Rayleigh waves, produced by the interaction of *P*- and *SV*-waves with the earth's surface layers, and Love waves, resulting from the interaction of *SH*-waves with these surface layers (Kramer 1996).

2.1.2 Site Amplification

As seismic waves propagate through the uppermost layers of soil and rock at a given site, these layers serve as a filter that can increase the duration and amplitude of earthquake shaking within a narrow frequency band (Molnar et al. 2004). The amplification of these waves is largely controlled by the mechanical properties of these layers.

2.1.2.1 Soil Sites

Amplification at sites with near-surface soil deposits is largely controlled by the density, shear-wave velocity, damping and thickness of these soils (Kramer 1996).

Typically, the densities (ρ) and shear-wave velocities (V_s) of the near-surface soil layers are smaller than those of the bedrock below. Since the energy contained in a seismic wave is proportional to $\rho V_s^2 A$ (where A is wave velocity amplitude), the amplitude of the wave tends to increase as it passes into the overlying layers, as a consequence of the need for conservation of energy (Archuleta et al. 1992). This type of amplification is often referred to as impedance contrast amplification (the impedance of a given material is the product of its density and seismic velocity, in this case - ρV_s).

The thicknesses of upper soil layers also influence site amplification. The resonant amplification of the amplitudes of seismic waves within a soil deposit is a function of the thickness and shear-wave velocity of its layers. This type of frequency-dependent amplification results from the reverberations of trapped shear-waves within the soil layers. The total thickness (h) and average shear-wave velocity (V_s) of these soil layers may be used to predict the first resonant peak, or fundamental frequency (f_0), of a soil deposit, as follows (Kramer 1996):

$$f_0 = \frac{V_s}{4h}. \tag{2.2}$$

The most significant site amplification can be expected at this frequency. Additional peaks may also occur at higher natural frequencies of the soil deposit (Kramer 1996). The impact of soil resonance on amplification is generally greater than that caused by impedance contrast (Siddiqqi 2000).

Another important soil characteristic that influences amplification of seismic waves is its damping. The seismic wave energy is dissipated through damping, resulting in a reduction in wave amplitude. Soil damping stems from two main mechanisms: radiation (due to propagation of seismic waves) and hysteretic (due to inelastic

deformation of soil), but are often lumped together so that they can be more conveniently represented (Kramer 1996). In geotechnical engineering, the soil damping is often described by its damping ratio (ξ).

Other factors, including topographic and subsurface irregularities, can also affect site amplification. Increased amplification, for example, has been noted near the crests of topographic ridges (e.g. Jibson 1987; Trifunac and Hudson 1971). Amplifications have also been shown to vary widely across alluvial valleys, due to the effects of basin geometry (e.g. King and Tucker 1984). Complex patterns of amplification and deamplification, caused by these irregularities, can significantly alter the characteristics of earthquake shaking. The two- and three-dimensional effects introduced by such features can be difficult to predict (Kramer 1996).

2.1.2.2 Rock Sites

Although the amplification of earthquake shaking by soil is well established, it is often assumed that hard-rock sites do not amplify ground motion (Siddiqqi and Atkinson 2002). Although not as pronounced as the amplification observed at soil sites, amplification at rock sites has been observed in a number of studies. Gupta and McLaughlin (1987), for example, show frequency-dependent amplification factors between 1.5 and 1.7 for sites in the eastern United States, while Siddiqqi and Atkinson (2002) found that average amplification factors for hard-rock sites in eastern Canada range from 1.1 and 1.5. Such amplification results from the impedance contrast caused by weathering of near-surface rock. Topographic effects have also been shown to influence amplification values at rock sites (Tucker et al. 1984).

2.2 EMPIRICAL EVALUATION

Empirical methods of site-effect evaluation attempt to develop site-response spectra from observed amplification measurements. Local site response is contained in these measurements, as indicated in Equation 2.1. In the frequency domain, the relationship between the observed amplitude (A) and site-response (S) spectra can be written as:

$$A(f) = E(f)P(f)S(f)I(f). \tag{2.3}$$

Generally, instrument response, I, is known, and therefore can be removed from the measured response with relative ease. The challenge for researchers then becomes removing source and path effects (E and P, respectively), so that local site response can be determined from these measurements (Field and Jacob 1995). Consequently, a number of empirical techniques have been developed to accomplish this task.

2.2.1 Standard Spectral Ratio Methods

Most commonly, source and path effects are removed from earthquake data using a method introduced by Borcherdt (1970), which divides the recorded spectrum at a given site (A_s) by one recorded at a nearby, bedrock reference site (A_b) (Molnar et al. 2004):

$$\frac{A_s(f)}{A_b(f)} = \frac{E_s(f)P_s(f)S_s(f)}{E_b(f)P_b(f)S_b(f)} \cong \frac{S_s(f)}{S_b(f)} \cong S_s(f). \tag{2.4}$$

The instrument response should be removed from both records prior to this calculation. This method relies on the assumptions that the two sites have similar source and path effects and that the reference site has negligible site amplification (i.e. $S_b \cong 1.0$) (Molnar et al. 2004).

The above technique, often referred to as the standard spectral ratio method, is limited by its dependence on the availability of an adequate reference site. In some areas, bedrock exposures may only exist at a considerable distance from the investigated site, making it difficult to assess the discrepancies related to the differing path effects at the two sites (Murphy 2003). Obtaining simultaneous records at both the soil and reference sites may also prove difficult (Lermo and Chavez-Garcia 1994). Soil-site amplification factors may also be affected by the inherent site-response of the reference site, even for a well-selected site on competent bedrock.

2.2.2 Borehole Methods

Perhaps the optimum bedrock reference, then, is that located directly below a given site (Archuleta et al. 1992). Boreholes may be drilled so seismometers can be placed at depths greater than the local geological conditions being studied. Spectral ratios can then be calculated between the surface and borehole seismograph recordings. Although accurate, this method can prove very costly, particularly in areas where variable near-surface conditions would necessitate multiple boreholes (Tsuboi et al. 2001).

2.2.3 Horizontal-to-Vertical Spectral Ratio Methods

The limitations of previously-discussed empirical techniques have spurred the development of alternatives that can determine site response in an efficient and cost-effective manner, even in the absence of an adequate reference site. An opportunity for this is provided by horizontal-to-vertical (H/V) spectral ratio methods. These methods

require only a single-station earthquake recording, and calculate site-response spectra by using the vertical component as reference (Molnar et al. 2004).

The primary assumption of the H/V spectral ratio techniques is that the vertical component is not influenced by resonant amplifications caused by local geology and thus, site response can be obtained by normalizing the vertical component from the horizontal component (Özel et al. 2002). In the frequency domain, this corresponds to the division of the horizontal spectrum, H, by the vertical spectrum, V, i.e.:

$$S(f) = \frac{H(f)}{V(f)} \tag{2.5}$$

where S is the local site response spectrum.

2.2.3.1 Nakamura's Method

Nakamura (1989) first proposed that the dynamic characteristics of near-surface structure could be estimated using the H/V ratios of microtremor measurements. Microtremors, low-period (up to 0.2 s) seismic noise, are attractive because their measurement can be readily accomplished. The background noise, which results from natural forces, such as storms and sea waves, as well as artificial forces, including industrial and cultural noise, can be obtained even in areas of low-seismicity (Murphy and Eaton 2005). Nakamura (1989) defined site response as the H/V ratio of surface noise, assuming that the vertical motion is not amplified by the near-surface structure.

Using surface microtremor measurements taken near the Kamonomiya, Tabata and Ishibashi train stations, in Japan, Nakamura (1989) approximated the transfer functions for each site from their H/V spectral ratios. Site-response spectra produced for

Kamonomiya were verified by comparison with ones produced using standard-spectral-ratio methods, while those produced for Tabata and Ishibashi were compared with the results of borehole methods. In all three cases, Nakamura (1989) concluded that the H/V spectral ratio provided a good estimate of the site-response spectra.

Since Nakamura's early work, his method has gained wide popularity. The method was successfully used to identify the fundamental frequency of sedimentary deposits (e.g. Field and Jacob 1993; Field and Jacob 1995; Lachet et al. 1996; Lermo and Chavez-Garcia 1994). Although Nakamura's (1989) method has been, in some cases, successful at providing a rough estimate of amplification level (e.g. Lermo and Chavez-Garcia 1994), it is generally observed to underpredict amplification values when compared with standard spectral ratio techniques (e.g. Field and Jacob 1995; Lachet et al. 1996).

2.2.3.2 HVSR Method of Lermo and Chavez-Garcia

Lermo and Chavez-Garcia (1993) attempted to apply Nakamura's technique to the *S*-wave portion of earthquake records. Their method is similar to the receiver-function technique used by Langston (1979) to determine crustal structure. They applied the technique to earthquake recordings from a number of seismograph stations in Mexico. For each station, the *S*-wave portion was extracted from earthquake records, and the transfer function computed from the horizontal-to-vertical spectral ratio (HVSR).

Spectra obtained using their method, herein referred to as the HVSR method, were compared with those computed from standard spectral ratios (see Equation 2.4). Their results indicate that the HVSR method can be used to estimate the frequency and

amplification of the first resonant mode, particularly when site effects are caused by relatively simple geology. Higher modes of amplification, however, are not predicted by this method. Further, their results suggest that site effects due to topographic features and sedimentary deposits could be well-predicted by this method (Lermo and Chavez-Garcia 1993).

There is significant empirical evidence that supports the use of the HVSR method in determining a site's fundamental frequency (e.g. Bonilla et al. 1997; Dimitiru et al. 1998; Field and Jacob 1995; Tsuboi et al. 2001). As with Nakamura's technique, debate exists as to whether it can accurately predict amplification values. Despite this limitation, both methods are useful in seismic hazard analysis, particularly since the identification of the fundamental frequency is typically of greatest concern.

2.3 NUMERICAL EVALUATION

Empirical methods, like those discussed above, predict the surface amplification at a given site. Although this data is necessary to the study of site response, subsurface amplification and stress information can also be useful. Obtaining such information can be accomplished with the use of numerical modelling. Additionally, numerical modelling can be employed to validate empirically-produced site-response spectra by comparison with theoretical spectra (e.g. Murphy and Eaton 2005). Furthermore, numerical modelling can provide theoretical support for the assumptions of empirical methods (e.g. Field and Jacob 1993). It can also be used to predict the response of a site to a large sample of possible input motions or to analyze various parameters which can affect site response (Lermo and Chavez-Garcia 1994).

2.3.1 Profile Data

Construction of an adequate model for site-response prediction requires detailed knowledge of the site near-surface characteristics. Soil layer thickness, shear-wave velocity and unit weight are among the geotechnical properties required to fully define the profile. Obtaining this data requires a site-investigation program, which often involves drilling boreholes or conducting shallow seismic refraction surveys.

Seismic-refraction profiling involves measuring the arrival times of the direct and refracted *P*- and/or *S*-waves as they travel from an impulse source to the points along a linear array (Kramer 1996). Refraction profiling has been used successfully to delineate near-surface structure in many cases (e.g. Beresnev and Atkinson 1997; Williams et al. 2003). A sledgehammer blow and five to seven stacks are often for recording relatively clear arrivals when acquiring relatively shallow depth data; however an explosive charge may be required to determine deeper crustal structure. Beresnev and Atkinson (1997) reported that a sledgehammer was an adequate source to determine the shear-wave velocity profile to a depth of approximately 70 m in their refraction study.

Velocity-structure data obtained in the course of model development can also be used to determine a site's National Earthquake Hazard Reduction Program (NEHRP) classification. The NEHRP classification scheme, described fully in the following section, forms the basis of the new National Building Code of Canada provisions related to local site effects.

2.3.1.1 National Building Code of Canada Provisions

Contemporary building code provisions developed to account for local site effects generally do so by adopting classification schemes which lump groups of similar soil profiles together (Kramer 1996). This is done in an attempt to incorporate local site effects into seismic design, without unduly complicating the structural design process (Finn and Wightman 2003).

The National Building Code of Canada (NBCC) (1995) grouped near-surface conditions into four categories, assigning a foundation factor, F, ranging from 1.0 to 2.0, to each category (See Appendix A, Table A.1). This classification scheme was often criticized for its use of broad and qualitative site categories (Finn and Wightman 2003). To address this concern, the NBCC (2005) adopted the classification scheme proposed by the National Earthquake Hazard Reduction Program (NEHRP 1994). The categories proposed by NEHRP (1994), detailed in Table 2.1, are defined quantitatively in terms of the weighted average shear-wave velocity of the top 30 m of the site, $\overline{V_{30}}$, average standard penetration resistance, $\overline{N}$, average undrained shear strength, $\overline{S_u}$, water content w, and plasticity index, PI. The use of such soil parameters eliminates much of the ambiguity associated with the earlier code (Finn and Wightman 2003). These site classes are used in the selection of design foundation factors, thus incorporating consideration for site effects into building design.

Table 2.1: Site classification for seismic site response (NEHRP 1994).

Site Class	Site class name and generic description	Site class definition
A	Hard rock	$\overline{V_{30}} > 1500$ m/s
B	Rock	$760 < \overline{V_{30}} < 1500$ m/s
C	Very dense soil and soft rock	$360 < \overline{V_{30}} < 760$ m/s, $\overline{N} > 50$, or $\overline{S_u} > 100$ kPa
D	Stiff soil	$180 < \overline{V_{30}} < 360$ m/s, $15 \leq \overline{N} \leq 50$, or $50 \leq \overline{S_u} \leq 100$ kPa
E	Soil profile with soft clay	$\overline{V_{30}} < 180$ m/s; PI > 20, $w > 40\%$, and $\overline{S_u} < 25$ kPa
F	Site-specific geotechnical investigations and dynamic site response analyses: (*i*) soils vulnerable to potential failure or collapse under seismic loading (liquefiable soils, quick and highly sensitive clays, collapsible weakly cemented soils, *etc.*); (*ii*) peats and (or) highly organic clays ($h > 3$ m of peat and (or) highly organic clay, where h is thickness of soil); (*iii*) very high plasticity clays ($h > 8$ m with PI > 75); (*iv*) very thick "soft - medium-stiff clays" ($h > 36$m)	

2.3.2 One-dimensional Modelling

When the near-surface structure, as determined by a site-characterization program, is relatively simple, site-response can often be computed using one-dimensional (1D) analyses. In such analyses, soil deposit conditions are idealized as horizontal layers of infinite extent (Bardet et al. 2000). Site response is assumed to result primarily from *SH*-waves propagating vertically from the underlying bedrock (Kramer 1996). 1D

analyses are suitable for modelling sites with level, or gently sloping ground with parallel material boundaries. Such conditions are not uncommon in engineering practice (Kramer 1996). In many cases, 1D procedures predict site response in good agreement with that determined empirically (e.g. Murphy and Eaton 2005; Triantafyllidis et al. 1999). However, this type of modelling is not appropriate for sites where major topographic or subsurface irregularities contribute to the site response and for strong earthquakes.

2.3.3 Nonlinear Site-Response

The nonlinear response of soil beyond a certain level of deformation has been well established (Kramer 1996); however, the necessity of incorporating this nonlinearity into site-response analysis is a somewhat contentious issue. It has long been a concern of geotechnical engineers, who recognized the nonlinear relationship of shear stress and strain in laboratory cyclic loading tests. On the other hand, it was rarely considered by seismologists due to the lack of nonlinear response observed in early records (Lee et al. 2006). However, as the number of permanent strong-motion arrays has increased in recent years, seismologists have seen greater evidence of nonlinear site-response in their observations. The debate regarding the inclusion of nonlinear behaviour in site-response modelling is well-summarized in a review by Beresnev and Wen (1996). They also listed several cases where linear-elastic models have reasonably predicted site response, and discussed several studies that provide evidence of nonlinear response. The review concluded that, generally, nonlinear site effects should be accounted for at high strain levels, particularly when softer soils are involved.

2.3.3.1 Equivalent-linear Modelling

Undertaking true nonlinear response analysis is both complicated and computationally demanding (Kramer 1996). For this reason, the nonlinear soil behaviour is often estimated using the more efficient equivalent-linear method. In the equivalent-linear approach, the analyses are performed assuming linear soil properties that are iteratively adjusted to be consistent with an effective level of shear strain induced in each soil layer (Arslan and Siyahi 2006; Molnar et al. 2004). This approximation requires that an equivalent-linear shear modulus (G_{sec}) and damping ratio (ξ) be specified, which are modified in response to computed strains. These strain-dependent properties are related to the hysteresis loop displayed by soil during cyclic loading (see Figure 2.2). Modulus-reduction and damping ratio curves, appropriate for modelling various soil types, have been established through experimentation (e.g. Vucetic and Dobry 1991).

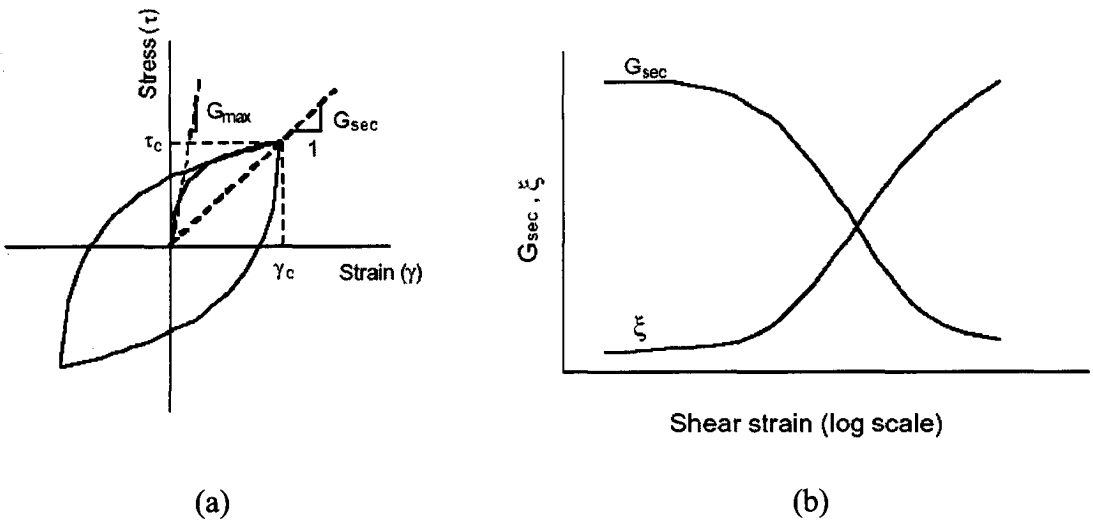

Figure 2.2: (a) Hysteresis stress-strain curve (G_{max} is small strain shear modulus) and (b) the variation of secant shear modulus and damping ratio with shear strain amplitude.

It should be noted that because of their inherent linearity, equivalent-linear analysis can only be viewed as an approximation of the actual nonlinear response. However, in instances where strain levels remain relatively low, such as in the cases involving stiff soil profiles or weak ground motion, this method produces reasonable results (Kramer 1996).

2.3.3.2 Nonlinear Modelling

An alternative to equivalent-linear analysis is using methods that incorporate true nonlinear representation of the soil behavior under high level strain loading. These methods calculate soil response using direct numerical integration in the time domain (Kramer 1996). One-dimensional nonlinear modelling analyses typically characterize the nonlinear stress-strain behaviour of soil using cyclic stress-strain models, such as the one proposed by Iwan (1967). The Iwan (1967) model is composed of linear springs and Coulomb friction elements, and can represent a broad range of nonlinear behaviour (Beresnev and Wen 1996). This cyclic stress-strain model is followed in small, incrementally linear, steps (Kramer 1996).

This type of analysis represents a more computationally-complex approach than that used by the equivalent-linear method. However it produces more accurate results in cases involving high levels of strain.

2.3.4 Modelling Programs

The interest in efficient and accurate modelling of local site effects has spurred the development of numerous site-response programs. The SHAKE program of Schnabel

et al. (1972) was one of the first programs produced for this purpose. The program implements the equivalent-linear method, and remains one of the most popular programs in geotechnical earthquake engineering (Bardet et al. 2000). It is often used as the standard to which newer modelling programs are compared. Such is the case for two, newer, equivalent-linear modelling programs: the Equivalent-linear site Response Analysis (EERA) program of Bardet et al. (2000) and the finite-element modelling program QUAKE/W 2004 (Krahn 2004).

EERA is a modern implementation of the equivalent-linear method, developed from the same basic concepts as SHAKE (Bardet et. al 2000). This 1D modelling program has the advantages of being freely available from the Internet, and being fully integrated with the spreadsheet program Microsoft Excel, making it convenient for practical use (Bardet et al. 2001). The program predictions compare favourably with those obtained from SHAKE, thus validating the program (Bardet et al. 2001). Additionally, EERA has been shown in several studies to successfully predict site-response in comparison to empirically-produced spectra (e.g. Murphy and Eaton 2005).

Like EERA, QUAKE/W (Krahn 2004) is a relatively new program that can be used for equivalent-linear modelling. Unlike EERA, QUAKE/W is not specifically designed for the prediction of site-response, but rather it is a finite element program that can be used to perform a variety of one- and two-dimensional dynamic analyses. In addition to its flexibility, this program offers the ability to integrate with programs slope-stability (SLOPE/W), seepage (SEEP/W), stress-deformation (SIGMA/W), and other analysis programs offered in its software suite. Although QUAKE/W is not currently as widely used as more-established programs like SHAKE, the potential offered by this

integration makes the study of its capabilities worthwhile. The program's developers offer some evidence that the program compares favourably with SHAKE for simple 1D analyses (Krahn 2004), however, further benefit could be derived from additional, independent comparisons.

While the above programs approximate nonlinear soil-response using the equivalent-linear method, the Nonlinear Earthquake site Response Analyses (NERA) of Bardet and Tobita (2001), uses the implementation principles of EERA, but applies them toward nonlinear analysis. The program can perform 1D ground response analysis using the material models developed by Iwan (1967) and Mroz (1967). Integration of the equations of motion is accomplished using the finite-difference method. Like EERA, the program is available for free and is integrated with Excel. While limited studies comparing these two programs are available in the literature (e.g. Bardet et al. 2001), further investigation and comparison of the programs is warranted to fully assess their capabilities.

REFERENCES

Archuleta, R. J., Seale, S. H., Sangas, P. V., Baker, L. M., and Swain, S. T. (1992). "Garner Valley downhole array of accelerometers: instrumentation and preliminary data analysis." *Bulletin of the Seismological Society of America*, 82(4), 1592-1621.

Arslan, H., and Siyahi, B. (2006). "A comparative study on linear and nonlinear site response analysis." *Environmental Geology*, 50(8), 1193-1200.

Bardet, J. P., Iichi, K., and Lin, C. H. (2000). *EERA: A Computer Program for Equivalent Linear Earthquake Site Response Analysis of Layered Soil Deposits*, University of Southern California, Department of Civil Engineering.

Bardet, J. P, and Tobita, T. (2001). *NERA: A Computer Program for Nonlinear Earthquake site Response Analyses of Layered Soil Deposits*, University of Southern California, Department of Civil Engineering.

Bardet, J. P., Tobita, T., Ichii, K., and Rogers, A. (2001). "Site response analysis at the vertical arrays of the Cerritos College Police Station and San Bernadino Main Fire Station." *A report to the USGS on Collaborative Research between GeoRisk Associates, Inc. and the University of Southern California*, University of Southern California, Department of Civil Engineering.

Beresnev, I., and Atkinson, G. M. (1997). "Shear wave velocity survey of seismographic sites in eastern Canada: calibration of empirical regression method of estimating site-response." *Seismological Research Letters*, 68(6), 981-987.

Beresnev, I. and Wen, K. (1996). "Nonlinear soil response - A reality?" *Bulletin of the Seismological Society of America*, 86(6), 1964-1978.

Bonilla, L.F., Steidl, J.H., Lindley, G.T., Tumarkin, A.G. and Archuleta, R.J. (1997). "Site amplification in the San Fernando Valley, California: variability of site-effect estimation using the S-wave, Coda, and H/V methods". Bulletin of the Seismological Society of America, 87 (3), 710-730.

Borcherdt, R. D. (1970). "Effects of local geology on ground motion near San Francisco Bay." *Bulletin of the Seismological Society of America*, 60(1), 29-61.

Dimitriu, P.P., Papaioannou, Ch. A. and Theodulidis, N.P. (1998). "EURO-SEISTEST strong-motion array near Thessaloniki, Northern Greece: a study of site effects". Bulletin of the Seismological Society of America, 88 (3), 862-873.

Field, E. H. and Jacob, K. H (1993). "The theoretical response of sedimentary layers to ambient seismic noise." *Geophysical Research Letters*, 20(24), 2925-2928.

Field, E. H. and Jacob, K. H. (1995). "A comparison and test of various site-response estimation techniques, including three that are not reference-site dependent." *Bulletin of the Seismological Society of America*, 85(4), 1127-1143.

Finn, L. W. D., and Wightman, A. (2003). "Ground motion amplification factors for the proposed 2005 edition of the National Building Code of Canada." *Canadian Journal of Civil Engineering*, 30(2), 272-278.

Gupta, I., and McLaughlin, K. (1987). "Attenuation of ground motion in eastern United States." *Seismological Society of America*, 77(2), 366-383.

Iwan, W. D. (1967). "On a class of models for the yielding behavior of continuous and composite systems." *Journal of Applied Mechanics*, 34, 612-617.

Jibson, R. (1987). "Summary of research on the effects of topographic amplification of earthquake shaking on slope stability." *Open-File Report 87-268*, U.S. Geological Survey, Menlo Park, California.

King, J.L., and Tucker, B.E. (1984). "Dependence of sediment-filled valley response on the input amplitude and the valley properties." *Bulletin of the Seismological Society of America*, 74(1), 153-165.

Krahn, J. (2004). *Dynamic Modelling with QUAKE/W: An Engineering Methodology,* GEO-SLOPE International Ltd., Calgary.

Kramer, S.L. (1996). *Geotechnical Earthquake Engineering*, Prentice Hall, New Jersey.

Lachet, C., Hatzfeld, D., Bard, P., Theodulidis, N., Papaioannou, C., and Savvaidis, A. (1996). "Site effects microzonation in the city of Thessaloniki (Greece) comparison of different approaches." *Bulletin of the Seismological Society of America*, 86(6), 1692-1703.

Langston, C. A. (1979). "Structure under Mount Rainier, Washington, inferred from teleseismic body waves." *Journal of Geophysical Research*, 84(B9), 4749-4762.

Lee, C., Tsai, Y., Wen, K. (2006). "Analysis of nonlinear site response using LSST downhole accelerometer array data." *Soil Dynamics and Earthquake Engineering,* 26(5), 435-460.

Lermo, J. F. and Chavez-Garcia, F. J. (1993). "Site effect evaluation using spectral ratios with only one station." *Bulletin of the Seismological Society of America*, 83(5), 1574-1594.

Lermo, J. F., and Chavez-Garcia, F. J. (1994). "Are microtremors useful in site-response evaluation?" *Bulletin of the Seismological Society of America*, 84(5), 1350-1364.

Molnar, S., Cassidy, J. F., and Dosso, S. E. (2004). "Site response in Victoria, British Columbia, from spectral rations and 1D modeling." *Bulletin of the Seismological Society of America*, 94(3), 1109-1124.

Mroz, Z. (1967). "On the description of anisotropic workhardening." Journal of Mechanics and Physics of Solids, 15, 163-175.

Murphy, C. (2003). "Near-surface characterization and estimated site response at POLARIS seismograph stations in southern Ontario, Canada." MSc thesis, University of Western Ontario, London, Ontario, Canada.

Murphy, C. and Eaton, D. (2005). "Empirical site response for POLARIS stations in Southern Ontario, Canada." *Seismological Research Letters*, 76(1), 99-109.

Nakamura, Y. (1989). "A method for dynamic characteristics estimation of subsurface using microtremor on the ground surface." *Quarterly Report of the Railway Technical Research Institute*, 30(1), 25-33.

NBCC (1995). *National Building Code of Canada 1995,* National Research Council of Canada, Ottawa, Ontario.

NBCC (2005). *National Building Code of Canada 2005,* National Research Council of Canada, Ottawa, Ontario.

NEHRP (1994). *1994 Recommended provisions for seismic regulations of new buildings: Part 1, provisions*, FEMA 222A, National Earthquake Hazard Reduction Program, Federal Emergencey Management Agency, Washington, D.C.

Özel, O., Cranswick, E., Meremonte, M., Erdik, M., and Safak, E. (1999). "Site effects in Avcilar, west of Istanbul, Turkey, from strong- and weak-motion data." *Bulletin of the Seismological Society of America*, 92(1), 499-508.

Parolai, S., Bormann, P., and Milkereit, C. (2002). "New relationships between V_S, thickness of sediments, and resonance frequency calculated by the H/V ration of seismic noise for the Cologne area (Germany)." *Bulletin of the Seismological Society of America*, 92(6), 2521-2527.

Schnabel, P.B., Lysmer, J., and Seed, H.B. (1972). "SHAKE: A Computer Program for Earthquake Response Analysis of Horizontally Layered Sites." Report No. UCB/EERC-72/12, Earhtquake Engineering Research Center, University of California, Berkley.

Siddiqqi, J. A. (2000). "Horizontal-to-vertical component ratios for earthquake ground motions recorded on hard rock sites in Canada." MSc thesis, Carelton University, Ottawa, Ontario, Canada.

Siddiqqi, J. and Atkinson, G. M. (2002). "Ground-motion amplification at rock sites across Canada as determined from the horizontal-to-vertical component ratio." *Bulletin of the Seismological Society of America*, 92(2), 877-884.

Trifunac, M. D., and Hudson, D. E. (1971). "Analysis of the Pacoima Dam accelerograms - San Fernando earthquake of 1971." *Bulletin of the Seismological Society of America*, 61(5), 1393-1411.

Triantafyllidis, P., Hatzidimitriou, P. M., Theodulidis, N., Suhadolc, P., Papazachos, C., Raptakis, D., and Lontzetidis, K. (1999). "Site effects in the City of Thessaloniki (Greece) estimated from acceleration data and 1D local soil profiles." *Bulletin of the Seismological Society of America*, 89(2), 521-537.

Tsuboi, S., Saito, M., and Ishihara, Y. (2001). "Verification of horizontal-to-vertical spectral-ratio technique for estimation of site response using borehole seismographs." *Bulletin of the Seismological Society of America*, 91(3), 499-510.

Tucker, B. E., King, J. L., Hatzfeld, D., and Nersesov, I. L. (1984). "Observations of hard-rock site effects." *Bulletin of the Seismological Society of America*, 74(1), 121-136.

Vucetic, M. and Dobry, R. (1991). "Effect of soil plasticity on cyclic response." *Journal of Geotechnical Engineering*, 117(1), 89-107.

Williams, R. A., Wood, S., Stephenson, W. J., Odum, J. K., Meremonte, M. E., Street, R., and Worleya, D. M. (2003). "Surface seismic refraction/reflection measurement determinations of potential site resonances and the areal uniformity of NEHRP Site Class D in Memphis Tennessee." *Earthquake Spectra*, 19(1), 159-189.

CHAPTER 3

EMPIRICAL SITE-RESPONSE SPECTRA

3.1 INTRODUCTION

Local geologic and soil conditions can greatly increase the intensity of earthquake ground shaking (Kramer 1996). These local site effects are particularly significant at sites with deep, soft soil deposits, although hard rock sites may also exhibit amplification (Siddiqqi and Atkinson 2002). Estimation of this localized site response can be accomplished using theoretical or empirical methods. Theoretical modelling requires extensive characterization of a site's near-surface geology, as well as the use of sophisticated computing methods. In contrast, empirical approaches require only ground motion data records from the site. The relative ease of application has popularized the use of empirical methods in investigating site response.

Ground motion records have become readily available at a number of Canadian sites, owing to the recent deployment, and subsequent expansion, of the POLARIS (Portable Observatories for Lithospheric Analysis and Research Investigating Seismicity) seismograph network (Eaton et al. 2005). In this study, empirical site-response spectra were produced for eleven stations of the POLO (POLARIS Ontario) array of the POLARIS seismograph network (Figure 3.1 and Table 3.1). A variety of near-surface conditions exist at these sites. While most are located on competent Precambrian bedrock, others rest on fractured Paleozoic bedrock, soil, or a combination of soil and man-made fill. Additionally the response spectrum at a station located on soil was also

studied (Figure 3.1 and Table 3.1). Installed near a cement quarry in St. Marys, Ontario, this seismic station (STM) collected data over a weeklong period.

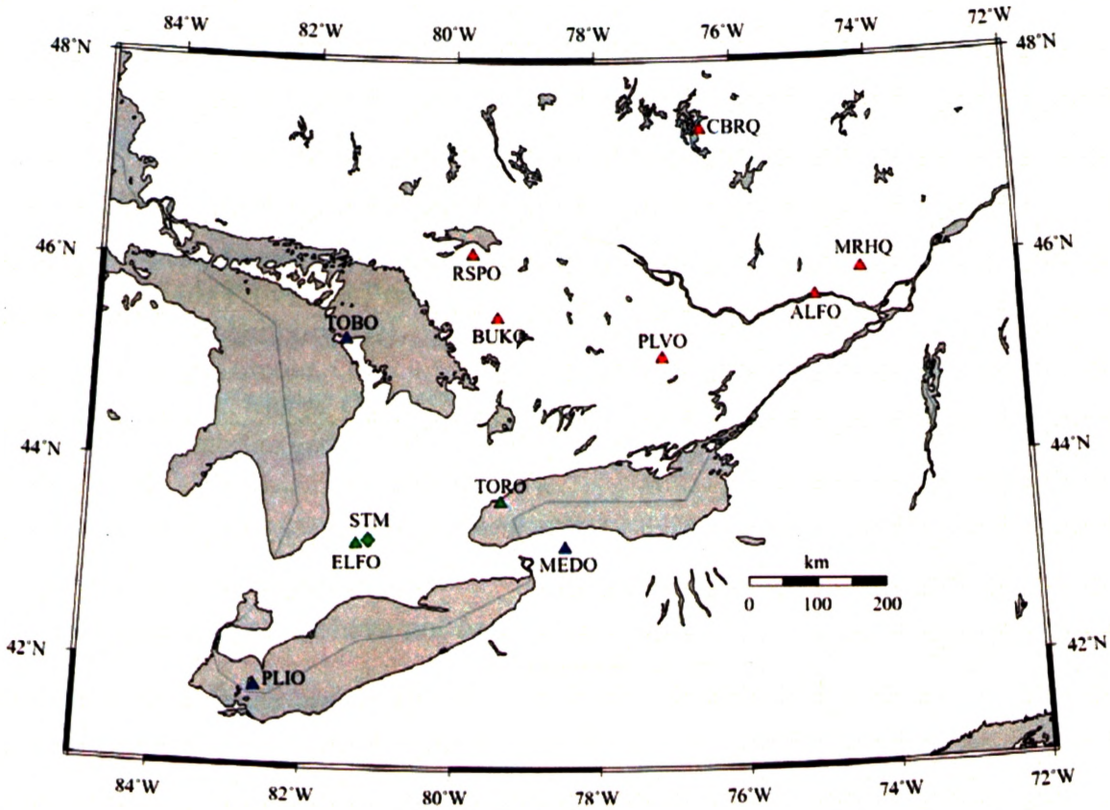

Figure 3.1: Seismograph stations used for this study. POLARIS stations located on Precambrian bedrock, Paleozoic bedrock and soil are indicated by red, blue and green triangles, respectively. The temporary soil station is indicated by a green diamond.

Table 3.1: Seismograph stations used for this study.

Station	Location	Latitude (°)	Longitude (°)	Elevation (m)	Type[1]
ALFO	Alfred, ON	45.62828	-74.88419	35	B
BUKO	Buck Lake, ON	45.44228	-79.39895	317	B
CBRQ	Cabonga Reservoir, QC	47.30915	-76.47073	307	B
ELFO	Elginfield, ON	43.19300	-81.31630	298	S
MRHQ	Morin Heights, QC	45.88700	-74.21270	422	B
MEDO	Medina, NY	43.16460	-78.45462	190	P
PLIO	Pelee Island, ON	41.75053	-82.62837	143	P
PLVO	Plevna, ON	45.03964	-77.07538	279	B
RSPO	Restoule Provincial Park, ON	46.07340	-79.76020	264	B
TOBO	Tobermory, ON	45.22573	-81.52337	169	P
TORO	Toronto, ON	43.61363	-79.34330	80	S
STM	St. Marys, ON	43.23606	-81.15272	314	S

[1]Type: B = Precambrian bedrock, P = Paleozoic bedrock, S = Soil.

The primary objective of this study was to report the site-response spectra for eleven POLO stations that have not been previously studied. Spectra produced in this study supplement those previously reported by Murphy and Eaton (2005) for eighteen other POLO stations. Two popular empirical methods were used to obtain the site-response spectra, allowing for a comparison of the results. The empirical methods employed were Nakamura's (1989) microtremor analysis method, and the horizontal-to-vertical spectra ratio (HVSR) method of Lermo and Chavez-Garcia (1993).

Additionally, theoretical site-response spectra were computed at the soil stations. Near-surface shear-wave velocity models were developed based on seismic refraction studies conducted at these sites (see Section 3.3.3). Spectra were then computed using the program EERA (Equivalent-linear Earthquake site Response Analyses), developed by Bardet et al. (2000), and used to validate those produced empirically.

3.2 EMPIRICAL ANALYSIS

Various empirical methods have been proposed for estimating site response. Spectral-ratio techniques, which are commonly used, calculate site amplification relative to a nearby, bedrock reference site. If an adequate reference site is not available, however, reference-site-independent techniques for determining site-response spectra can be particularly attractive. In these single-station methods, the horizontal-component spectrum of ground motion is divided by the corresponding vertical-component spectrum to estimate the amplification, thus using the vertical component as reference.

Both Nakamura (1989) and Lermo and Chavez-Garcia (1993) found that site response could be estimated from the ratio of the horizontal-to-vertical (H/V) component of the Fourier amplitude spectrum of ground motion. Nakamura (1989) originally proposed that this technique be applied to measurements of microtremors, low-period ambient seismic noise resulting from natural and artificial sources. Lermo and Chavez-Garcia (1993) later applied Nakamura's technique to the *S*-wave portion of earthquake records. They found that the frequency and amplitude of the first resonant mode could be estimated using this method, although higher modes were not evident.

These techniques have since been applied by various researchers, with varying degrees of success. Generally, it is agreed that these H/V techniques provide good estimates of the frequency of the first resonant mode at soil sites (Molnar et al. 2004; Field and Jacob 1995). H/V techniques have also provided reliable rough estimates of amplification level at sites with simple near-surface geologies (Tsuboi et al. 2001; Lermo and Chavez-Garcia 1994). Here, Nakamura's (1989) technique and the HVSR technique

of Lermo and Chavez-Garcia (1993) are applied to ground motion data records obtained from the POLO stations.

3.2.1 Ground Motion Data

A database of digital seismograms was compiled from ground motion velocity recordings (which were converted to accelerations using the program SAC) made at the eleven POLO stations over a 12-month period, beginning July 1, 2004. The stations are equipped with three-component broadband seismometers (Guralp CMG-3ESP Compact), digitizers and satellite systems (Nanometrics Libra VSAT), which record and transmit data, in near-real time, to acquisition centers in London and Ottawa, Ontario (Murphy and Eaton 2005). In addition to microtremor recordings, the database contained sixty-seven local and regional earthquakes of magnitude (m_N) 2.0 or greater. A complete list of the events selected for use in this study is included in Appendix B (Table B.1).

The temporary station (STM) was equipped with a three-component Guralp CMG-40T seismometer and a Nanometrics ORION digitizer, from which data were extracted. Recordings were made over a week-long period, beginning November 21, 2005. Only noise data were obtained, as no events were recorded during the station's operation.

At all stations, data were sampled at 100 Hz.

3.2.2 Nakamura's Method

For use in Nakamura's method, fifty noise windows, of 20 s duration, were extracted from the POLO and temporary station data. Noise windows were cosine

tapered (5%) and processed to produce Fourier spectra. The horizontal spectrum (H) was computed from the N-S (h_{NS}) and the E-W (h_{EW}) component spectra as follows (Yu and Haines 2003):

$$H(f) = \sqrt{h_{NS}{}^2(f) + h_{ES}{}^2(f)} \quad (3.1)$$

The horizontal and vertical Fourier spectra were smoothed over frequency increments of 0.2 Hz using a moving-average filter (0.4 Hz width), before they were used to compute H/V ratios. Normalizing the horizontal spectra by the vertical spectra effectively removes the instrument response from the record, as both components have identical instrument response (Siddiqqi and Atkinson 2002). MATLAB code written for the calculation of these spectra appears in Appendix C. The results of this analysis are plotted in Figure 3.2, with plots grouped according to near-surface type.

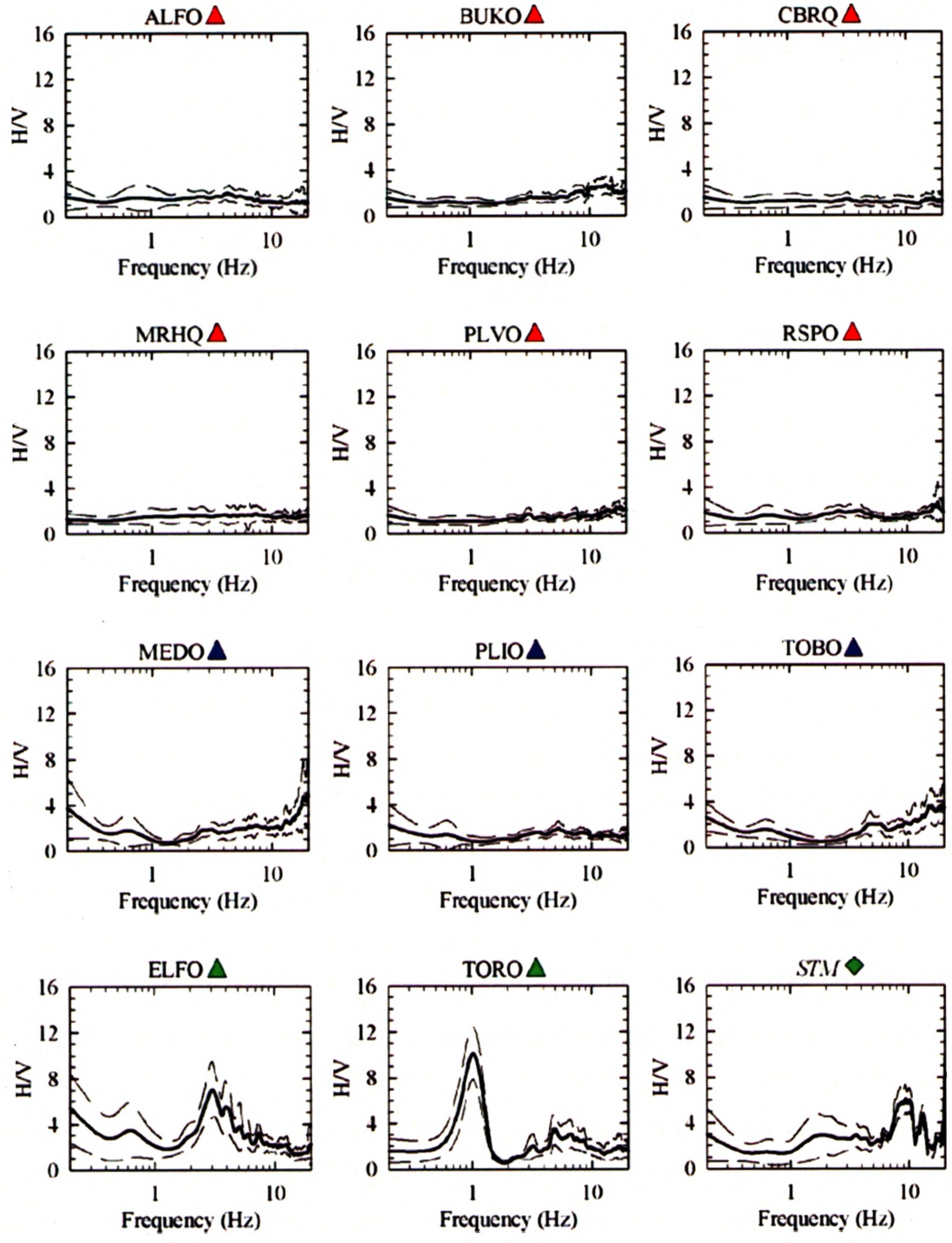

Figure 3.2: Empirical site-response spectra obtained using Nakamura's (1989) method. Mean amplification (thick, continuous line) ± one standard deviation (dashed lines). Station symbols are as in Figure 3.1.

A strong correlation between near-surface conditions and the shape of the site-response spectra is evident in the results presented in Figure 3.2. Precambrian bedrock sites (red triangles) exhibit an almost frequency-independent response, with mean amplification values between 1.2 and 2.0. The response at Paleozoic bedrock sites (blue triangles) is also relatively flat, but exhibits a higher degree of variability than the Precambrian bedrock sites, with mean amplification values ranging from 1.3 to 2.5. Soil sites (ELFO, TORO, STM) are characterized by a single resonant peak within the frequency-band considered. The peak amplification predicted by Nakamura's method at ELFO, TORO and STM occurs at 3.0, 1.0 and 9.4 Hz, respectively, with corresponding peak amplitude ratios of 7.0, 10.1 and 6.1. Higher resonant modes were not observed using this method.

3.2.3 HVSR Method of Lermo and Chavez-Garcia

The HVSR method of Lermo and Chavez-Garcia (1993) was applied to recordings of sixty-seven earthquake events of m_N between 2.0 and 3.8. At stations where an event was recorded, *S*-wave windows, 20-70 s long, starting at the *S*-wave arrival and containing the strongest portion of the earthquake records, were extracted. For each event, a pre-event noise window, of approximately the same length, was also extracted to be used in signal-to-noise ratio (SNR) calculations.

Processing of the signal and noise windows included 5% cosine-tapering and Fourier transformation. Horizontal signal and noise spectra were computed using Equation 3.1. After smoothing over frequency increments of 0.2 Hz, the H/V ratio was calculated for all frequencies at which signal-to-noise ratio exceeded 2.0 for both the

horizontal and vertical components. The selection of 2.0 as the threshold value was based on testing, and is supported by values in the literature (Murphy and Eaton 2005; Siddiqqi and Atkinson 2002). Gaps in the individual site-response spectra correspond to poor signal-to-noise ratios. MATLAB code written for the calculation of these spectra appears in Appendix C.

Plots of results, arranged by near-surface type, are presented in Figure 3.3. Note that the method could not be applied to data from the temporary station (STM), due to a lack of event recordings. This highlights one of the inherent disadvantages of using the HVSR method in areas of low to moderate seismicity.

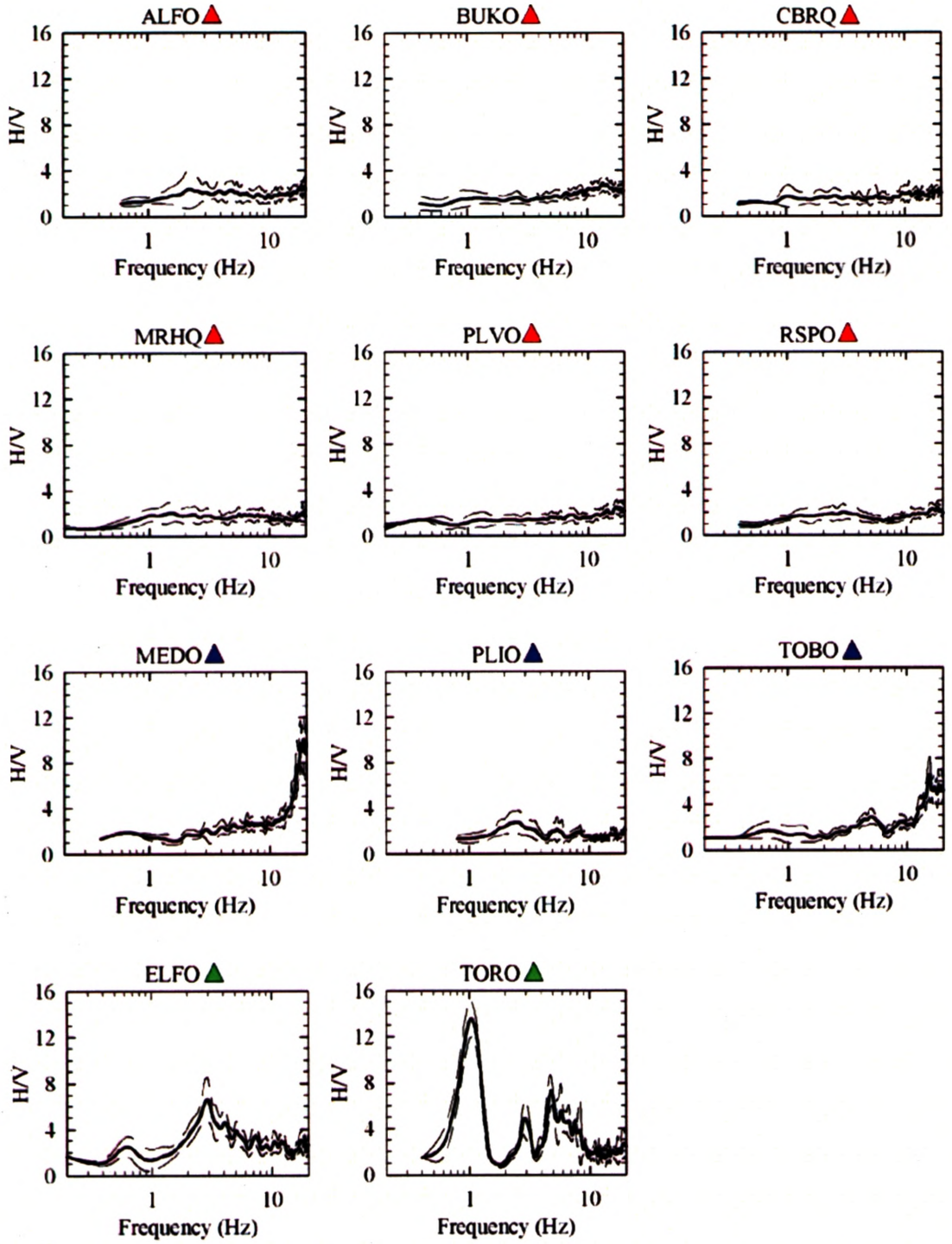

Figure 3.3: Empirical site-response spectra obtained using the HVSR method of Lermo and Chavez-Garcia (1993). Mean amplification (thick, continuous line) ± one standard deviation (dashed lines). Station symbols are as in Figure 3.1.

3.2.4 Comparison of the results

Results obtained with the HVSR method were in good agreement with those produced using Nakamura's method. Frequency-independent amplification predicted at the rock sites using the HVSR method was only slightly higher than that predicted using Nakamura's method. For comparison, the amplification values for the rock sites at 1 and 5 Hz, obtained using both methods, have been summarized in Table 3.2.

Table 3.2: Summary of H/V ratios obtained at rock sites.

Station	Type[1]	Nakamura's Method		HVSR Method	
		1 Hz	5 Hz	1 Hz	5 Hz
		Mean H/V	Mean H/V	Mean H/V	Mean H/V
ALFO	B	1.58 ± 0.99	1.74 ± 0.52	1.33 ± 0.30	2.22 ± 0.82
BUKO	B	1.14 ± 0.38	1.48 ± 0.34	1.55 ± 0.69	1.69 ± 0.38
CBRQ	B	1.22 ± 0.59	1.11 ± 0.44	1.71 ± 0.95	1.55 ± 0.68
MRHQ	B	1.50 ± 0.72	1.58 ± 0.65	1.84 ± 0.56	1.75 ± 0.41
PLVO	B	1.12 ± 0.43	1.32 ± 0.31	1.17 ± 0.57	1.60 ± 0.50
RSPO	B	1.31 ± 0.56	1.52 ± 0.31	1.48 ± 0.24	1.45 ± 0.40
MEDO	P	0.98 ± 0.46	1.94 ± 0.80	1.48 ± 0.28	2.60 ± 0.67
PLIO	P	0.83 ± 0.40	1.77 ± 0.45	1.33 ± 0.40	1.98 ± 0.83
TOBO	P	0.93 ± 0.54	2.05 ± 0.75	1.31 ± 0.73	2.88 ± 0.64
Average		1.18 ± 0.25	1.61 ± 0.30	1.47 ± 0.21	1.97 ± 0.50

[1]Type: B = Precambrian bedrock, P = Paleozoic bedrock.
Uncertainties show ± one standard deviation.

Similar amplification values were predicted by both methods. Average amplification values obtained at 1 and 5 Hz are in good agreement with those predicted by Siddiqqi and Atkinson (2002) for eastern Canada and by Gupta and McLaughlin (1987) for the eastern United States.

Nakamura's method and the HVSR method also produced similar predictions of the frequency of the first resonant peak at the two soil sites. Further discussion of the soil-site results is contained in a subsequent section (Section 3.3.3).

3.3 SITE RESPONSE MODELLING

Simple numerical models can be used to predict site-response spectra, given that sufficient information about the site's near-surface geology is available. In this study, numerical spectra were produced for the three soil sites (ELFO, TORO, STM) for comparison with those determined from empirical estimates. For modelling purposes, it was necessary to obtain or estimate the relevant geotechnical properties of the near-surface layers at these sites.

3.3.1 Refraction Data Collection and Processing

Little information was known about the near-surface conditions at ELFO and TORO, while at STM, some borehole information was available. Therefore, hammer-seismic refraction surveys were conducted at the three soil stations (ELFO, TORO, STM) to determine their near-surface velocity structures.

For each survey, a steel I-beam struck at 45° by a sledgehammer that was used as the source. The I-beam was set up in-line with the profile, and the *SH*-waves produced were recorded by a spread of 4.5-Hz horizontal geophones. Details of the geophone spreads used at each site are included in Table 3.3. At ELFO, the survey was conducted using two lines of geophones, oriented perpendicular to one another, while a single line of geophones was used at both TORO and STM, due to topographic constraints at these sites. Forward and reverse profiles were conducted along each line, so the data could later be examined for evidence of dipping of the near-surface layer boundaries.

Table 3.3: Geophone spreads used in this study.

Station	Line	Source Offset(s) (m)	Number of Geophones	Geophone Spacing (m)
ELFO	1	1, 30	24	5
	2	1, 30	24	5
TORO	1	5	12	10
STM	1	15	12	10

At each site, digital seismograms from source impacts were stacked ten times and stored in data files created using a seismic-refraction software package (Geometrics 2004). Acquisition polarity was then reversed by striking the I-beam on the opposite side, and the procedure was repeated. After transferring the data to a computer, the difference between the normal and reverse polarity traces at each geophone was calculated to enhance the *S*-wave arrivals and suppress the *P*-wave arrivals (Lankston 1990). Figure 3.4a shows an example of the resulting traces, with *S*-wave arrivals clearly visible. Arrival times identified from the traces were plotted versus source-receiver distances, as in Figure 3.4b, for use in subsequent analysis.

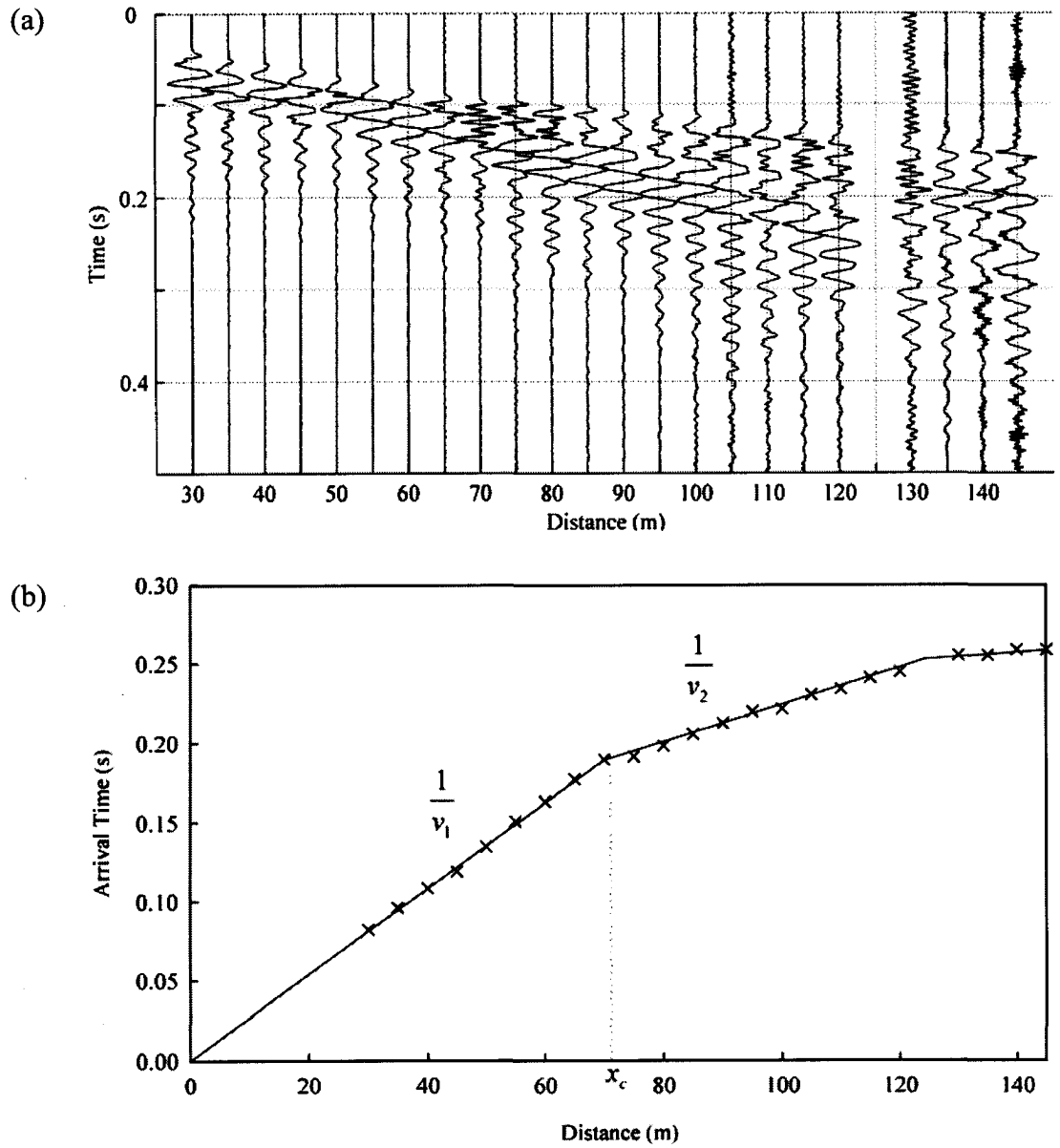

Figure 3.4: (a) Sample trace data collected at ELFO. (b) Corresponding time-distance plot, showing v_1, v_2 and x_c.

3.3.2 Velocity-model Construction

Following the procedure of the U.S. Corps of Engineers (1979), the time-distance plots were interpreted to produce the one-dimensional (1D) velocity models. Using this method, the thickness, H, of the uppermost soil layer was calculated as follows:

$$H = \frac{x_c}{2}\sqrt{\frac{v_2 - v_1}{v_2 + v_1}}, \tag{3.2}$$

where v_1 and v_2 are the velocities of first and second soil layers and x_c is the critical distance. Velocities were calculated from the inverse slopes of best-fit lines applied to the time-distance plots, while the critical distance corresponds to the break in slope between these two best-fit lines (see Figure 3.4b). For all deeper soil layers, thicknesses were calculated using:

$$H_k = \frac{x_{ck}}{2}\sqrt{\frac{v_{k+1} - v_k}{v_{k+1} + v_k}} + \sum_{j=1}^{k-1}\frac{H_j}{v_j}\frac{v_{k+1}\sqrt{v_k^2 - v_j^2} - v_k\sqrt{v_{k+1}^2 - v_j^2}}{\sqrt{v_{k+1}^2 - v_k^2}} \quad (k \geq 2) \tag{3.3}$$

where H_k is the thickness of the kth layer.

Profiles were also examined to determine the dip angle in the near-surface layers. Because no significant dipping of these layers was found along any of the profiles, they could be represented as simple, one-dimensional cross-sections with horizontal layering. Beresnev and Atkinson (1997) noted that for the south and southeast Ontario region, the velocity structure can be determined to a depth of approximately 70 m using this type of refraction setup. This was also found to be the approximate depth of penetration in this study. The models produced are plotted, for the upper 70 m, in Figure 3.5.

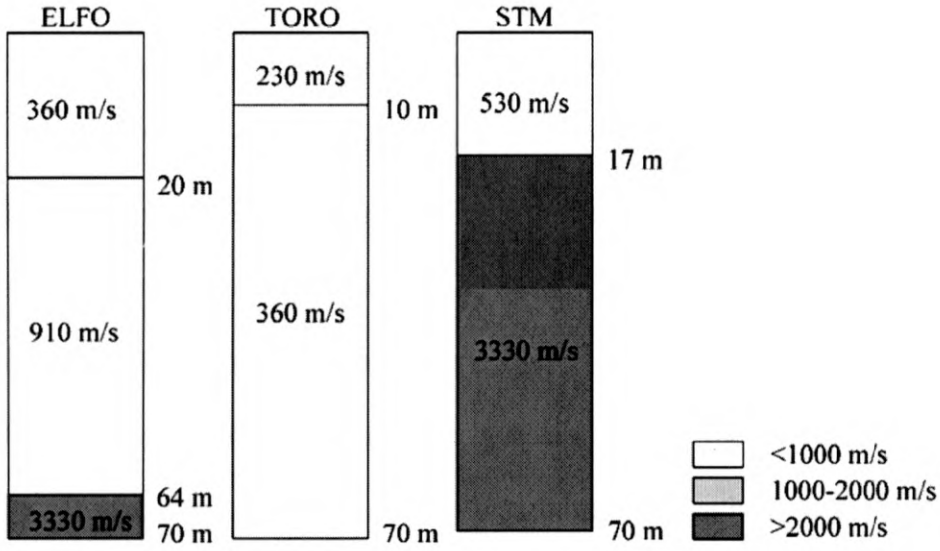

Figure 3.5: Soil columns based on refraction data. The average layer depths and shear-wave velocities are indicated.

3.3.3 Numerical Modelling

Numerical analysis was performed using the EERA program of Bardet et al. (2000), which computes the response in a horizontally layered soil-rock system subjected to transient and vertically traveling shear waves. The velocity profiles were used to build the numerical models to calculate the theoretical site-response spectra. The April 20, 2002 Au Sable Forks earthquake (m_N=5.1), in upstate New York, was used as the input motion. This ground acceleration record was extracted from a nearby bedrock station in Kingston, Ontario (KGNO Canadian National Seismographic Network).

To completely define the soil profiles, it was necessary to specify a unit weight and damping values. Because relatively weak ground motions are being modelled, a linear model can be used to predict the response (Shearer and Orcutt 1987). As a result,

frequency-independent damping ratios were specified. Bedrock layers were assigned a unit weight of 27.5 kN/m^3 and 0% damping, and soil layers were assigned a unit weight of 17.7 kN/m^3 and 1.667% damping. These properties were adopted based on those used in similar studies conducted in the south and southeast Ontario region (Murphy and Eaton 2005; Beresnev and Atkinson 1997). The soil at STM was assigned a unit weight of 22.0 kN/m^3 based on available borehole data.

At TORO, the depth to bedrock could not be established by the refraction survey (see Figure 3.5). It was, therefore, necessary to determine this depth through iterative modelling. Consequently, the depth of the second soil layer (V_s=360 m/s) was extended to a depth of 90 m. Below this depth, a rock layer with the properties of the bedrock found at ELFO and STM, was assumed.

The results of this numerical modelling are plotted in Figure 3.6, and summarized in Table 3.4. The National Earthquake Hazards Reduction Program (NEHRP) classification for each site is also included in Table 3.4 (BSSC 2003). Further details of this classification system can be found in Chapter 2 (Section 2.3.1.1).

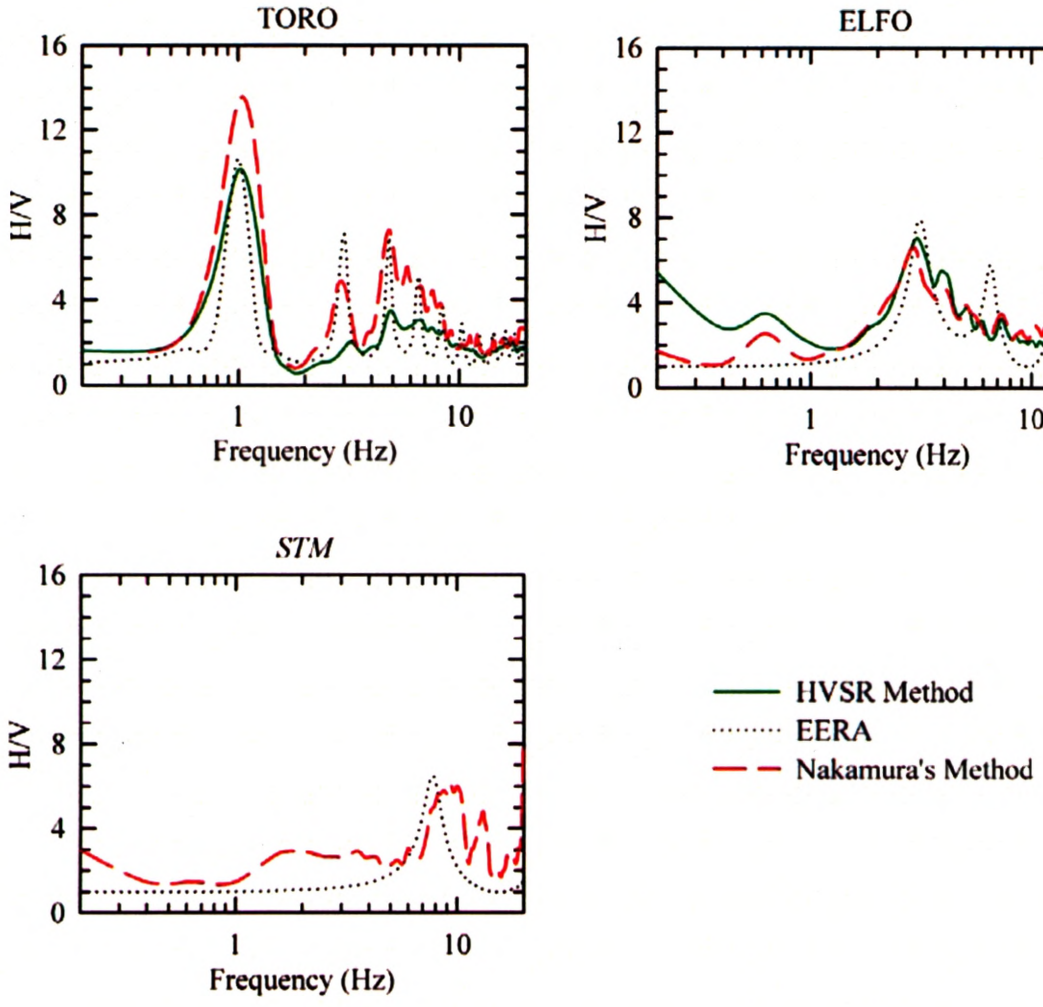

Figure 3.6: Empirical and numerical site-response spectra at soil sites produced using Nakamura's method, the HVSR method and numerical methods in EERA.

Table 3.4: Summary of empirical and numerical site-response parameters at soil sites.

Station	NEHRP Site Class[1]	Theoretical		Nakamura's Method		HVSR Method	
		f_0 (Hz)	A	f_0 (Hz)	A	f_0 (Hz)	A
ELFO	C	3.2	7.7	3.0	7.0	2.8	6.5
TORO	D	1.0	10.7	1.0	10.1	1.0	13.3
STM	B	7.8	6.5	9.4	6.1		

[1]See Chapter 2, Section 2.3.1.1

f_0 is the frequency of fundamental or first resonant mode.

A is the peak amplitude ratio of the fundamental or first resonant mode.

Theoretical spectra contain a peak at the fundamental frequency (f_0), determined by the average shear-wave velocity of the soil layers (V_S) and the total thickness of these layers (h), i.e.:

$$f_0 = \frac{V_S}{4h}. \tag{3.4}$$

At TORO and ELFO, harmonic overtones were predicted by the models, in the frequency range of interest.

At all three sites, frequencies of the resonant peaks produced by the empirical methods agreed well with the fundamental frequencies predicted numerically. This suggests the refraction surveys have correctly determined the shear-wave velocities and thicknesses of the soils at these sites. Overall, the empirical and theoretical methods predicted similar values for peak amplification, although it should be noted amplification determined numerically is highly dependent on the assumed damping ratios.

At TORO, the HVSR method appears to have predicted the higher harmonic modes. In all other cases, these overtones were not observed in the empirical spectra. These overtones, typical of simple, numerically produced spectra, result from the assumed linearity of the analysis (Shearer and Orcutt 1987). The absence of these modes in the empirical spectra likely reflects some nonlinear soil behaviour.

3.4 CONCLUSIONS

Empirical site-response spectra have been produced for eleven stations of the POLO network with variable near-surface conditions. Two H/V ratio techniques were employed in the study, namely: Nakamura's (1989) method and the HVSR method of Lermo and Chavez-Garcia (1993). The shapes of the resulting spectra were observed to

correlate with the site's near-surface type. Hard rock sites exhibited response spectra that were relatively frequency-independent, with Nakamura's method predicting an average amplification of 1.2 ± 0.3 at 1 Hz, increasing to 1.6 ± 0.3 at 5 Hz. The HVSR method, generally, produced slightly higher estimates of amplification, with an average of 1.5 ± 0.2 at 1 Hz, increasing to 2.0 ± 0.5 at 5 Hz. The amplifications predicted are in line with those predicted at other hard rock sites in eastern North America. In contrast, response spectra at soil sites were characterized by a prominent spectral peak at the fundamental frequency. At all stations, the strong agreement between both empirical methods was notable.

Simple 1D linear models were used to produce response spectra at the three soil sites. The theoretical results support the notion that the fundamental resonance mode can be reliably obtained using H/V ratio methods. In one case (TORO), higher modes of resonance also appear to have been predicted by the HVSR method.

REFERENCES

Bardet, J. P., Iichi, K., and Lin, C. H. (2000). *EERA: A Computer Program for Equivalent Linear Earthquake Site Response Analysis of Layered Soil Deposits*, University of Southern California, Department of Civil Engineering.

Beresnev, I., and Atkinson, G. M. (1997). "Shear wave velocity survey of seismographic sites in eastern Canada: calibration of empirical regression method of estimating site-response." *Seismological Research Letters*, 68(6), 981-987.

Building Seismic Safety Council (BSSC) (2003). *2003 NEHRP recommended provisions for seismic regulations for new buildings and other structures with accompanying commentary,* FEMA 450, developed for the Federal Emergency Management Agency, Washington, 46-49.

Eaton, D., Adams, J., Asudeh, I., Atkinson, G. M., Bostock, M. G., Cassidy, J. F., Ferguson, I. J., Samson, C., Snyder, D. B., Tiampo, K. F., and Unsworth, M. F. (2005). "Investigating Canada's Lithosphere and Earthquake Hazards with Portable Arrays." EOS, *Transactions of the American Geophysical Union*, 86(17), 169-176.

Field, E. H. and Jacob, K. H. (1995). "A comparison and test of various site-response estimation techniques, including three that are not reference-site dependent." *Bulletin of the Seismological Society of America*, 85(4), 1127-1143.

Geometrics (2004). *Geometrics Multiple Geode OS*, Geometrics, San Hose, California.

Gupta, I., and McLaughlin, K. (1987). "Attenuation of ground motion in eastern United States." *Seismological Society of America*, 77(2), 366-383.

Kramer, S.L. (1996). *Geotechnical Earthquake Engineering*, Prentice Hall, New Jersey.

Lankston, R. W. (1990). "High-resolution refraction seismic data acquisition and interpretation." *Geotechnical and Environmental Geophysics, Vol. 1: Review and Tutorial*. ed.. Ward, S. H., Society of Exploration Geophysicists, Tulsa, 45-73.

Lermo, J. F. and Chavez-Garcia, F. J. (1993). "Site effect evaluation using spectral ratios with only one station." *Bulletin of the Seismological Society of America*, 83(5), 1574-1594.

Molnar, S., Cassidy, J. F., and Dosso, S. E. (2004). "Site response in Victoria, British Columbia, from spectral rations and 1D modeling." *Bulletin of the Seismological Society of America*, 94(3), 1109-1124.

Murphy, C. and Eaton, D. (2005). "Empirical site response for POLARIS stations in Southern Ontario, Canada." *Seismological Research Letters*, 76(1), 99-109.

Nakamura, Y. (1989). "A method for dynamic characteristics estimation of subsurface using microtremor on the ground surface." *Quarterly Report of the Railway Technical Research Institute*, 30(1), 25-33.

Shearer P. M., and Orcutt, J.A. (1987). "Surface and near-surface effects on seismic waves-theory and borehole seismometer results." *Bulletin of the Seismological Society of America,* 77(4), 1168-1196.

Siddiqqi, J. and Atkinson, G. M. (2002). "Ground-motion amplification at rock sites across Canada as determined from the horizontal-to-vertical component ratio." *Bulletin of the Seismological Society of America*, 92(2), 877-884.

Tsuboi, S., Saito, M., and Ishihara, Y. (2001). "Verification of horizontal-to-vertical spectral-ratio technique for estimation of site response using borehole seismographs." *Bulletin of the Seismological Society of America*, 91(3), 499-510.

CHAPTER 4

NUMERICAL MODELLING

4.1 INTRODUCTION

Numerical modelling software packages provide a useful tool for the investigation of site response, accounting for the localized amplification of earthquake motion due to the near-surface geology. Numerical models that are based on information related to the site near-surface layers can be used to produce theoretical site-response spectra, which quantitatively represent this amplification.

Employing modelling techniques that are capable of accounting for the nonlinearity of this response can be necessary for accurate site-response prediction, particularly when soft soils or strong ground motions are involved (Beresnev and Wen 1996). Numerical modelling programs typically account for this nonlinear behaviour using either equivalent-linear approximations or true nonlinear analysis. While the former is more computationally convenient, it is limited in its ability to produce reasonable estimates of ground response at higher strain levels (Kramer 1996).

In this study, the performance of three computer programs that are used to predict site response is evaluated. Two of these programs utilize the equivalent linear approach: the Equivalent-linear Earthquake Response Analysis (EERA) program of Bardet et al. (2000), and the finite-element modelling program QUAKE/W 2004 (Krahn 2004). The third program, the Nonlinear Earthquake site Response Analysis (NERA) program of Bardet and Tobita (2001), employs the nonlinear method. These programs were used to produce theoretical site-response spectra at five sites in Southern Ontario, Canada. At

each site, ground response to synthetic earthquakes, representative of low-, moderate- and high-intensity Canadian earthquakes was calculated. Comparison of the computed theoretical spectra was undertaken to assess the ability of these programs to model site response to earthquakes of various intensities.

4.2 SITE SELECTION

The sites used in this study are the locations of several stations from the POLARIS (Portable Observatories for Lithospheric Analysis and Research Investigating Seismicity) seismograph network. Research related to this Ontario stations (e.g. Beresnev and Atkinson 1997; Murphy 2003; and see Chapter 3) has produced near-surface profiles and related data for many of these stations. Since this investigation involves modelling the nonlinear response of soil, five sites revealed to have near-surface soils were chosen from the available profiles. The locations of the five selected sites can be found in Figure 4.1 and Table 4.1.

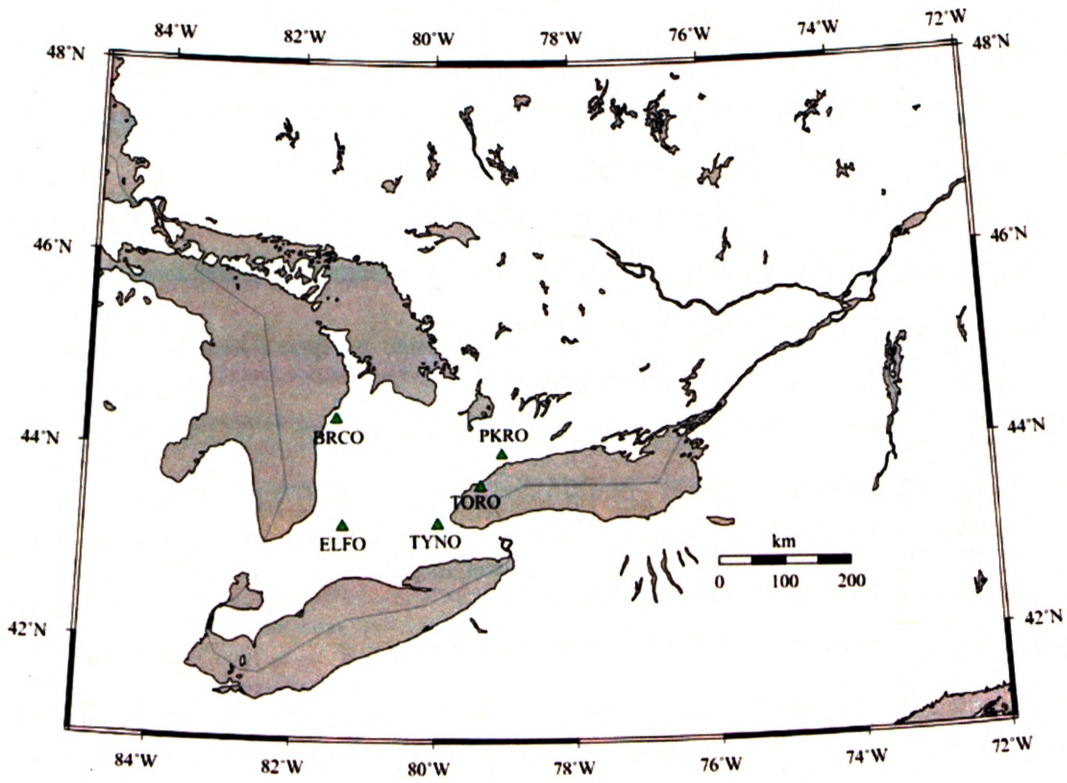

Figure 4.1: POLARIS stations sites used in this study.

Table 4.1: Locations of POLARIS station sites used in this study.

Station	Location	Latitude (°)	Longitude (°)	Elevation (m)
BRCO	Bruce Peninsula, ON	44.24372	-81.44225	273
ELFO	Elginfield, ON	43.19300	-81.31630	298
PKRO	Pickering, ON	43.96431	-79.07143	197
TORO	Toronto, ON	43.61363	-79.34330	80
TYNO	Tyneside, ON	43.09498	-79.97018	205

4.3 NUMERICAL MODELLING

4.3.1 Modelling Programs

Three computer programs were used to analyze potential site amplification at the five POLARIS sites: EERA, NERA and QUAKE/W. EERA (Equivalent-linear

Earthquake site Response Analysis) is a one-dimensional (1D) modelling program, developed by Bardet at al. (2000) to compute the response of a horizontally layered, soil-rock system to vertically travelling shear waves using the equivalent linear method.

The equivalent-linear method follows an iterative procedure, whereby an initial shear modulus (G) and damping ratio (ξ) are assumed and used to compute the ground response and corresponding shear strains for each layer. Effective shear strain is then calculated as a percentage (typically between 50 and 70%) of the maximum shear strain computed for the time history. Here, effective shear (γ_{eff}) was calculated as:

$$\gamma_{eff} = R_\gamma \gamma_{\max} \tag{4.1}$$

where γ_{max} is the maximum shear strain and R_γ is the ratio of effective shear strain, defined as:

$$R_\gamma = \frac{M-1}{10} \tag{4.2}$$

where M is earthquake magnitude (Idriss and Sun 1992). New values for G and ξ, corresponding to this level of effective shear strain, are then chosen, and the process is repeated until the differences are reduced below a certain tolerance level, in this case, 1% (Kramer 1996).

QUAKE/W (Krahn 2004) also has equivalent-linear modelling capabilities; however it is fundamentally different in its formulation. QUAKE/W is a finite-element modelling program and, as such, may be used to model a variety of soil configurations. One-dimensional modelling can be readily accomplished with this program, provided models are constructed with the appropriate boundary conditions.

NERA (Nonlinear Earthquake site Response Analysis) of Bardet and Tobita (2001) is a one-dimensional ground-response modelling program similar to EERA,

however, it employs nonlinear analysis. Nonlinear analysis uses direct numerical integration in the time domain to calculate the soil response. NERA uses an Iwan (1967)-type cyclic-stress strain model, where soil is modelled as a series of springs and frictional elements. The program performs integration in the time domain using the finite-difference method.

As its name suggests, EERA primarily functions to model site response. The program can be used to produce site-response spectra directly. QUAKE/W, because of its inherent flexibility, does not readily produce such spectra. Acceleration time histories at the ground surface, however, can be extracted directly from QUAKE/W. It was, therefore, necessary in this study to compute QUAKE/W theoretical spectra from these time histories. A similar procedure was followed to calculate the NERA spectra.

4.3.2 Soil Profile Data

To completely define the profiles in each of the programs, the thickness of each layer is required, as well as the relevant values for soil shear-wave velocity, unit weight and damping for each layer.

Shear-wave velocity profiles for three of the stations (BRCO, PKRO, TYNO) were obtained from Beresnev and Atkinson (1997). The profiles for the remaining stations (ELFO, TORO) were produced by the author (see Chapter 3, Section 3.3). These profiles are presented in Figure 4.2. Given these soil profiles, it is possible to obtain the National Earthquake Hazard Reduction Program (NEHRP) classification for each of these sites (see Chapter 2, Section 2.3.1.1). ELFO, PKRO and TORO are representative of NEHRP Class C sites, while BRCO and TYNO are site class D (NEHRP 1994).

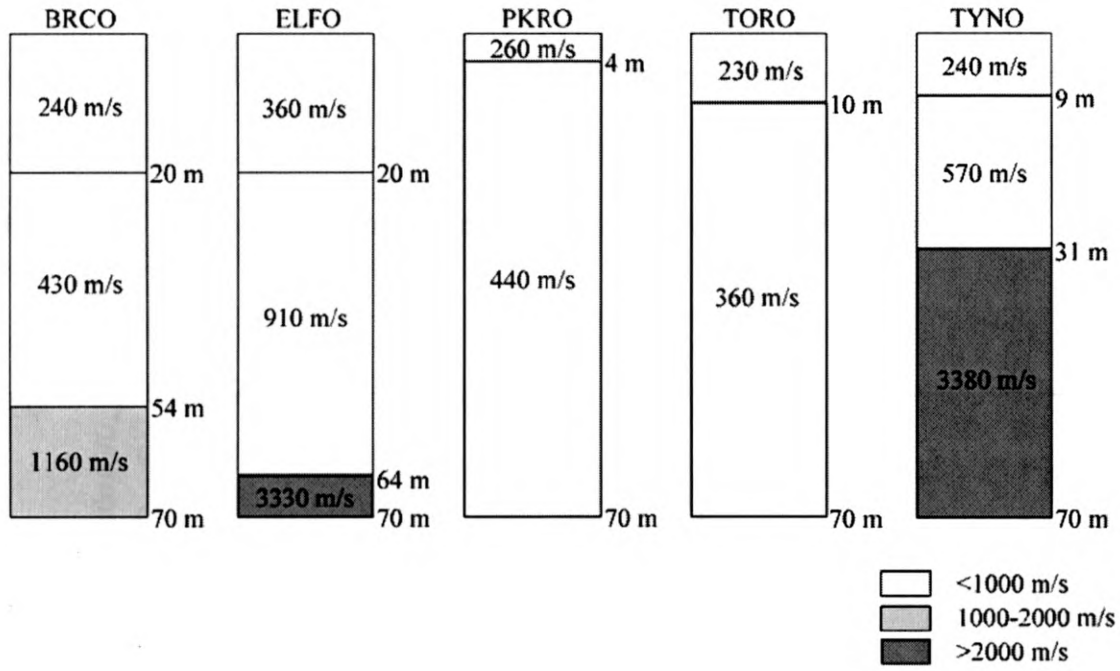

Figure 4.2: Shear-wave velocity profiles used in this study (BRCO, PKRO, TYNO after Beresnev and Atkinson 1997).

The soil unit weight was assigned based on soil type, with values adopted from similar studies conducted in the south and southeast Ontario region (Beresnev and Atkinson 1997; Murphy and Eaton 2005). Soil layers with $V_s < 1000$ m/s (see Figure 4.2) were assigned a unit weight, $\gamma_s = 17.7$ kN/m^3. BRCO's rock layer ($1000 < V_s < 2000$ m/s) was assigned a unit weight, $\gamma_s = 24.5$ kN/m^3. Layers with $V_s > 2000$ m/s were assumed to be bedrock, and assigned a unit weight, $\gamma_s = 27.5$ kN/m^3, the average for Precambrian crust in this region (Atkinson and Sommerville 1994). For profiles where bedrock was not encountered, a crustal layer was assigned directly below the upper 70 m.

Shear modulus and damping ratio curves were also assigned to each layer based on soil classification. For the equivalent-linear programs (EERA, QUAKE/W), soil layers were assigned the modulus reduction and damping curves provided by Sun et al. (1988), for $10 < PI < 20$. The modulus reduction and damping curves of Schnabel et al. (1970) were assigned to the rock layer. These curves are depicted in Figure 4.3.

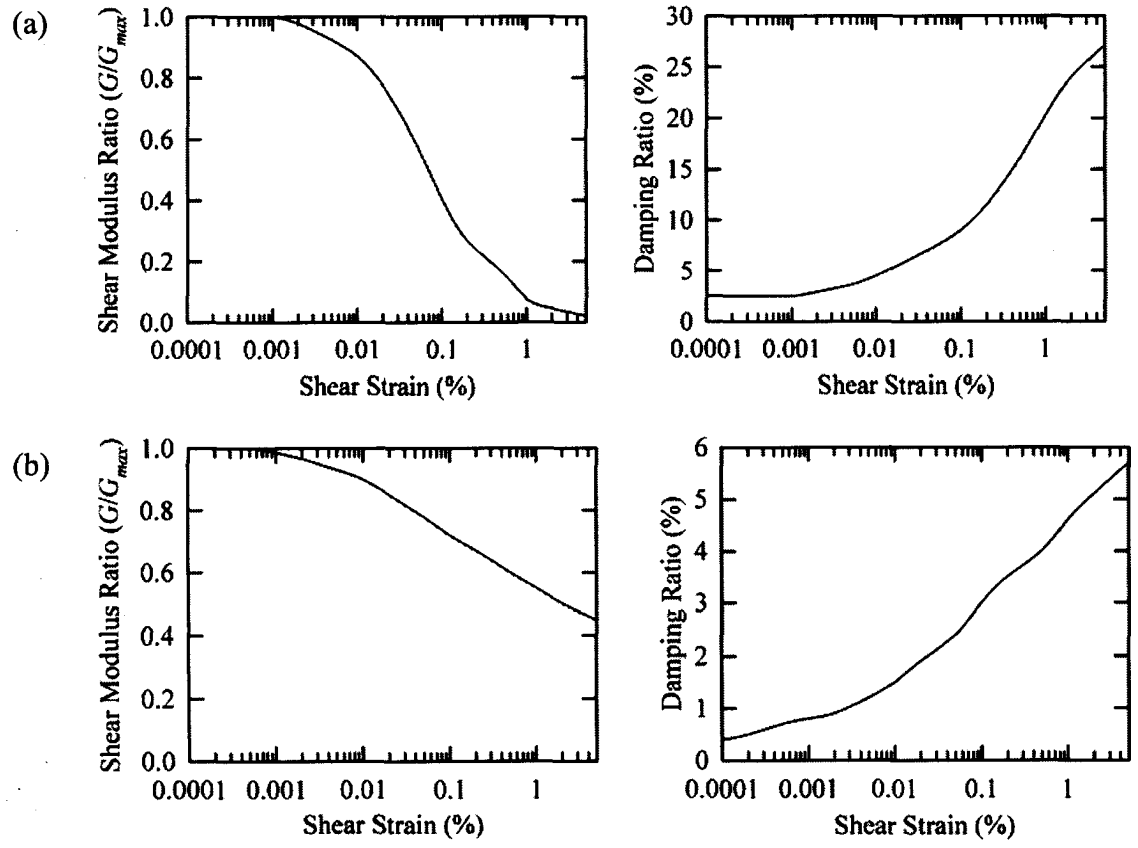

Figure 4.3: Modulus reduction and damping curves specified for (a) soil (Sun et al. 1988) and (b) rock (Schnabel et al. 1970).

For nonlinear modelling in NERA, only the modulus curves were specified, as NERA calculates the damping ratio based on the model proposed by Iwan (1967) and Mroz (1967).

4.3.3 Input Earthquake Motion

Ground motion records, used as input for the analyses, were selected from a suite of synthetic earthquake time histories produced by Atkinson (1999). This ensemble of input time histories was produced to be compatible with the Uniform Hazard Spectra (UHS), for "firm soil" conditions, used in the 2005 edition of the National Building Code of Canada (NBCC 2005). Earthquakes were simulated, for various moment magnitude (M) and distance (R) combinations, using the method described in Atkinson and Beresnev (1998). To match events experienced by various Canadian cities, it is necessary to extract earthquakes having appropriate magnitude-distance combinations from this suite, and multiply them by a recommended scale factor. For this study, earthquakes matching ground motions modelled for Toronto, Montreal and Victoria, intended to represent low, moderate and high levels of seismic input, respectively, were used. The magnitude, distance and scale factors corresponding to these earthquakes appear in Table 4.2. For Toronto, only one event-scenario is required to represent the seismic hazard. On the other hand, representing the seismic hazard for Montreal and Victoria requires both a short- and long-period events. The M8.5 Cascadia scenario listed in Table 4.2 simulates a mega-thrust earthquake on the Cascadia subduction zone.

Table 4.2: Magnitude-distance combinations and scale factors of earthquake events.

City	Short-period event	Scale Factor	Long-period event	Scale Factor
Toronto	$M = 6.0$ at $R = 50$ km	0.75	-	-
Montreal	$M = 6.0$ at $R = 30$ km	0.85	$M = 7.0$ at $R = 70$ km	0.90
Victoria	$M = 6.5$ at $R = 30$ km	1.20	$M = 8.5$ Cascadia	2.20

A single event for each scenario was extracted from the simulated earthquakes, and modified according to the scale factor. The resulting peak ground acceleration (PGA) of each earthquake used is listed in Table 4.3.

Table 4.3: PGA of the simulated earthquake records used in this study.

City	Short-period event	Long-period event
Toronto	0.155 g	-
Montreal	0.400 g	0.271 g
Victoria	0.640 g	0.238 g

4.3.3.1 Outcrop Motion

As mentioned previously, the EERA program of Bardet et al. (2000), and the NERA program of Bardet and Tobita (2001) are developed exclusively for 1D site-response analysis. Because earthquake accelerations are usually recorded at the ground surface, these programs are designed to treat earthquake records entered as, what are sometimes known as, "outcrop" records. Outcrop records are so-called because they are measured at the surface, where bedrock is outcropping, rather than at the soil-bedrock interface. This motion is modified by the program to reflect the motion at the soil-bedrock interface (i.e. deconvolution) and soil surface acceleration is then calculated based on this modified motion.

Figures 4.4 presents both the original and deconvolved motion for the Toronto earthquake at ELFO. Note that this deconvolution produces a slight decrease in the wave amplitude of the earthquake motion.

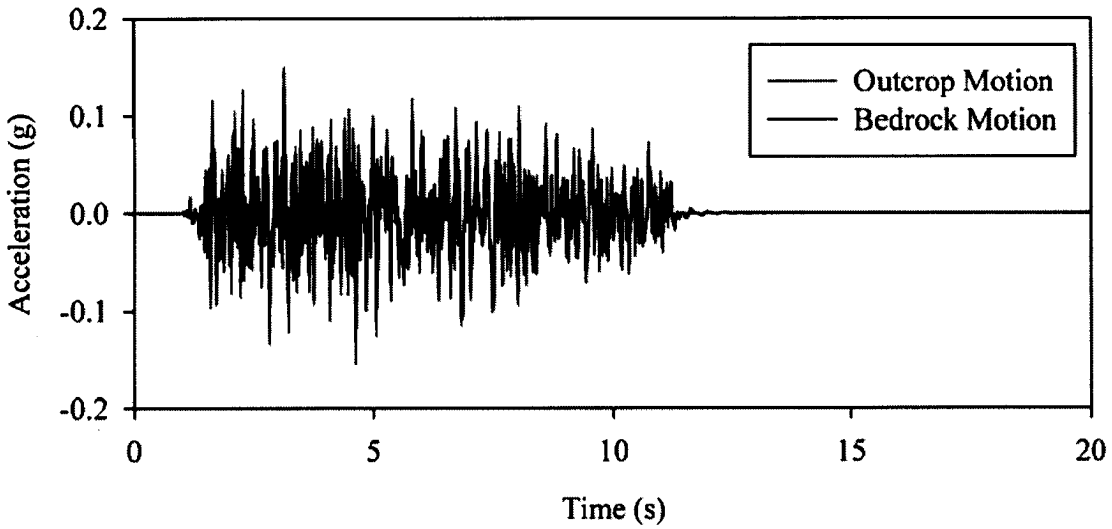

Figure 4.4: Original and deconvolved motion at ELFO.

While the deconvolution of outcropping motion can be readily accomplished by the 1D modelling programs, it is not explicitly encoded in the program QUAKE/W (Krahn 2004). To accommodate this, but still allow for direct comparison between the different programs, the modified soil-interface records produced by EERA for each earthquake were used as input for the QUAKE/W simulation.

4.3.4 Results and Discussion

Site-response spectra, representing the amplification of the surface motion relative to the bedrock outcropping motion, were calculated, for the five sites, using EERA, NERA and QUAKE/W. EERA-produced spectra were extracted directly from the

program, while for NERA and QUAKE/W the spectra were calculated from acceleration time histories.

The theoretical site-response spectra produced for the five POLO sites, plotted from 0 to 15 Hz, appear in Figures 4.5 to 4.9. A complete tabulation of all calculated values of all fundamental frequencies (f_0) and their associated amplification values (A), can be found in the Appendix D of this report.

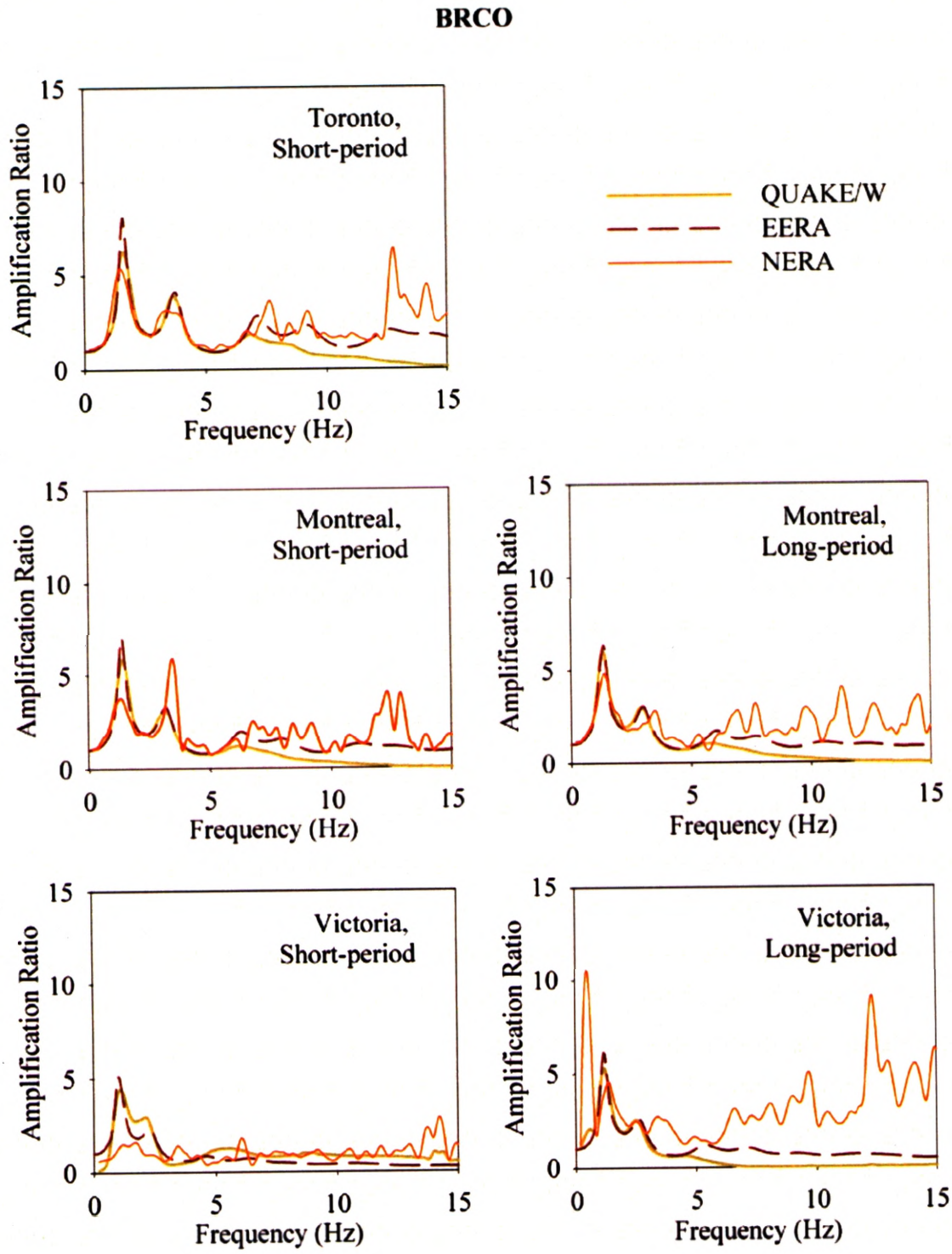

Figure 4.5: Site-response spectra predicted, for various earthquakes, at BRCO.

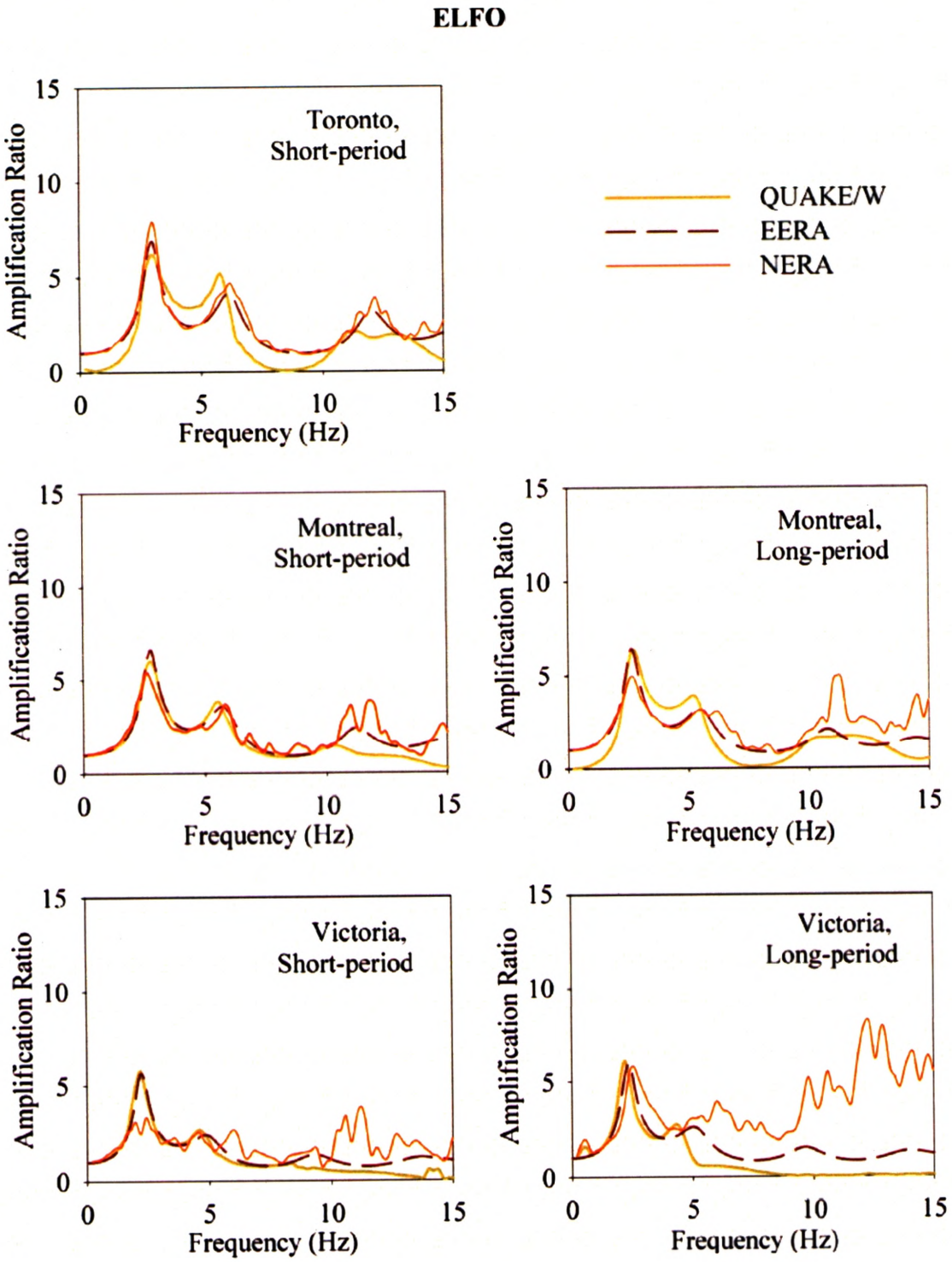

Figure 4.6: Site-response spectra predicted, for various earthquakes, at ELFO.

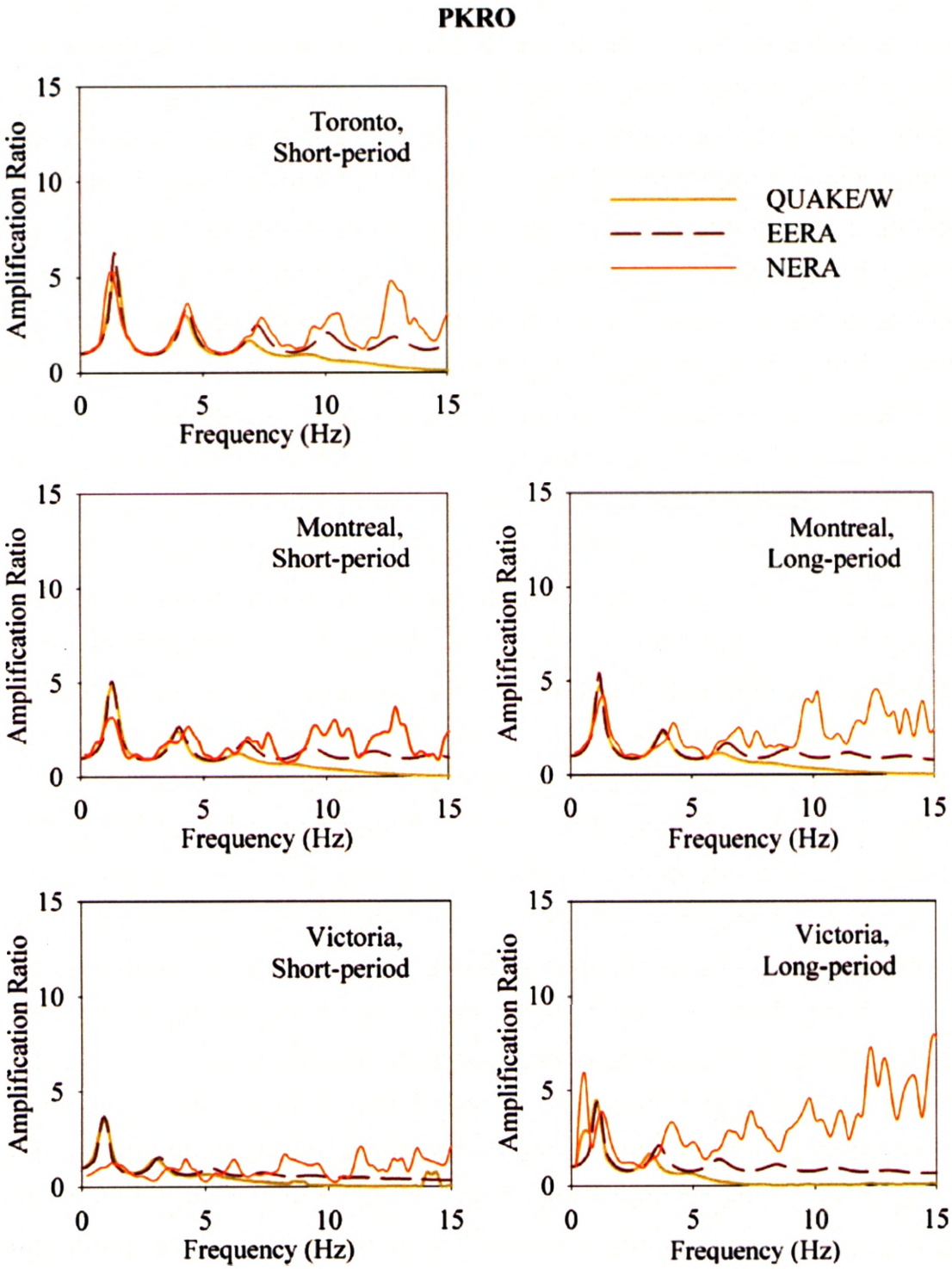

Figure 4.7: Site-response spectra predicted, for various earthquakes, at PKRO.

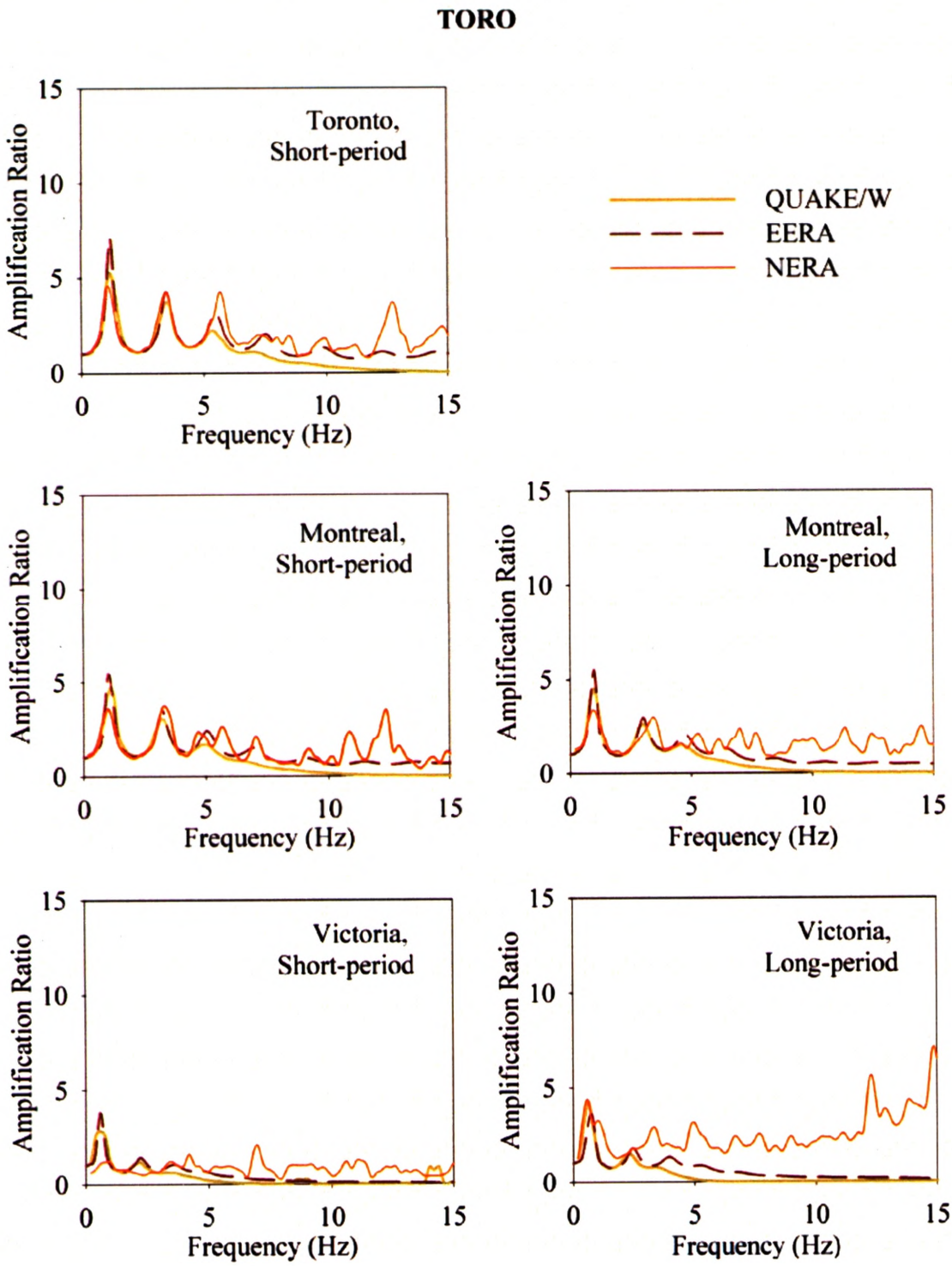

Figure 4.8: Site-response spectra predicted, for various earthquakes, at TORO.

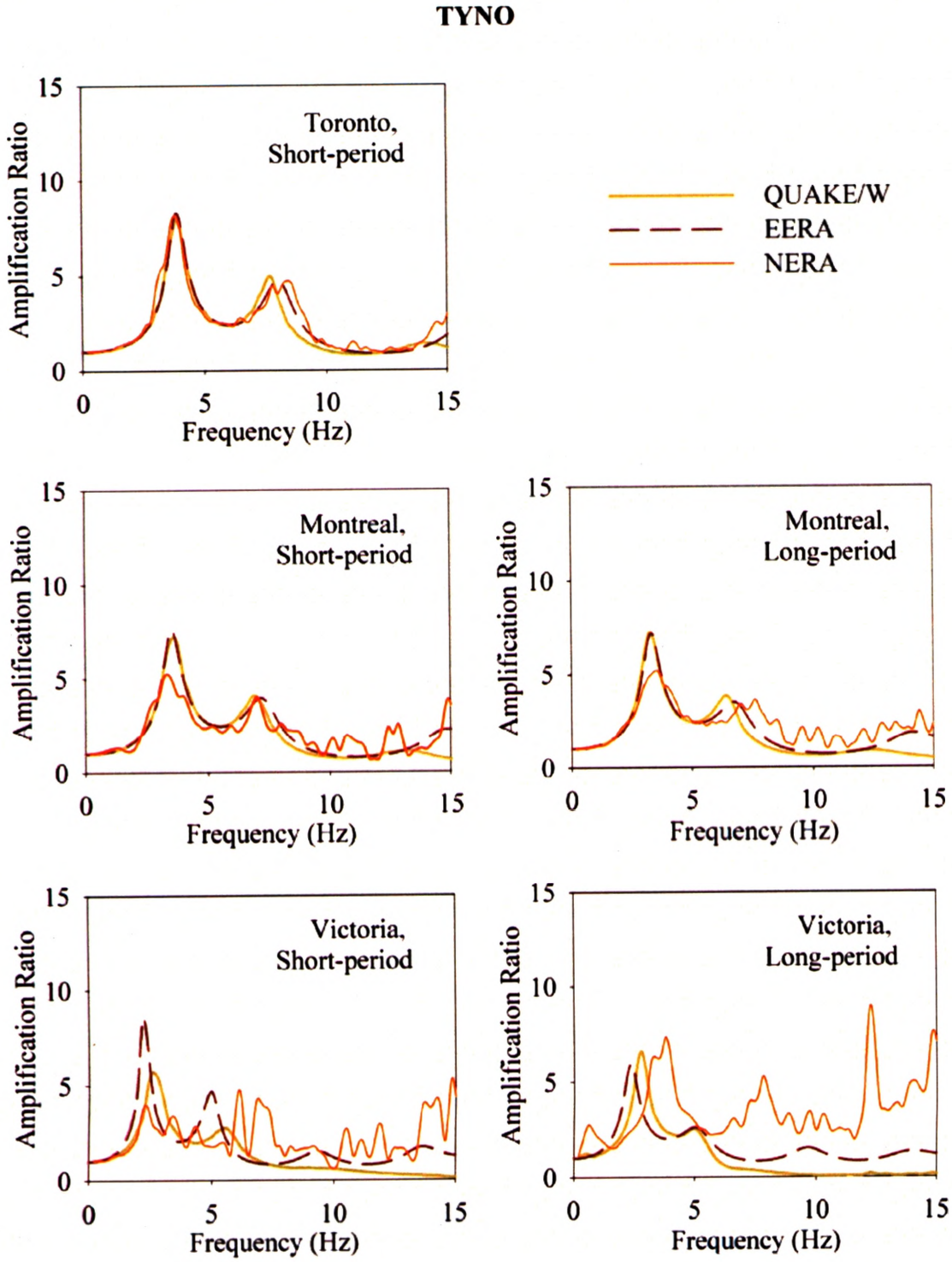

Figure 4.9: Site-response spectra predicted, for various earthquakes, at TYNO.

Comparison of spectra produced by all three programs shows generally good agreement in terms of the prediction of site-response spectra for the Toronto and Montreal earthquakes, which represent low- to moderate-intensity earthquakes. For this level of excitation, EERA, QUAKE/W and NERA all predict similar values for each site's fundamental frequency. At higher frequencies, however, QUAKE/W predicts lower amplification values than both NERA and EERA. Although QUAKE/W is not specifically designed for site-response, comparison with independently-developed programs, for relatively simple analyses such as these, can be used to verify whether the program has been coded correctly (Krahn 2004). Although the low-frequency agreement between the three programs is encouraging, the discrepancy at higher frequencies could, possibly, point to a formulation process that filters out the high frequency component of the ground motion in QUAKE/W.

As expected, for the higher-intensity Victoria earthquakes, the equivalent-linear programs (EERA, QUAKE/W) differ from the nonlinear program (NERA) in their site-response predictions. Differences in spectra are observed across the entire frequency band, but are most notable at higher frequencies, where NERA predicts higher amplification than the other two programs. As a result of the higher levels of strain induced by the stronger Victoria earthquakes, the equivalent-linear programs fail to accurately approximate this response.

Inspecting the site-response spectra for all sites considered reveals a trend related to the fundamental frequency (f_0), or lowest natural frequency, present in the response-spectra produced by all three programs. Generally, as earthquake intensity increases, a decrease in f_0 is observed. At BRCO, for example, f_0 values of 1.6 Hz, 1.4 Hz and 1.0 Hz

are predicted for the Toronto, Montreal and Vancouver short-period earthquakes, respectively, as shown in Figure 4.10.

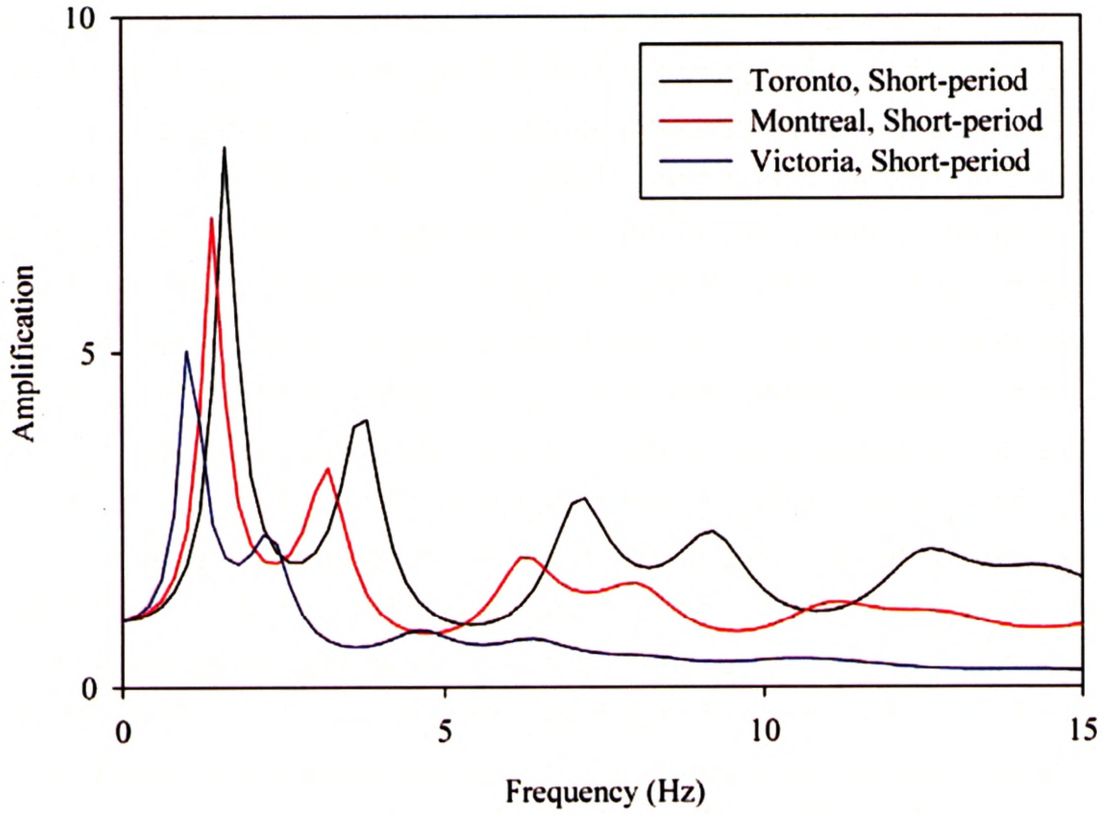

Figure 4.10: Amplification predicted at BRCO predicted by EERA.

The fundamental frequency is proportional to the average shear-wave velocity (V_s) of the upper soil layers as shown in Equation 4.3:

$$f_0 = \frac{V_S}{4h} \tag{4.3}$$

At increased strain levels, soils experience a reduction in the effective shear modulus (G), as shown in Figure 4.11.

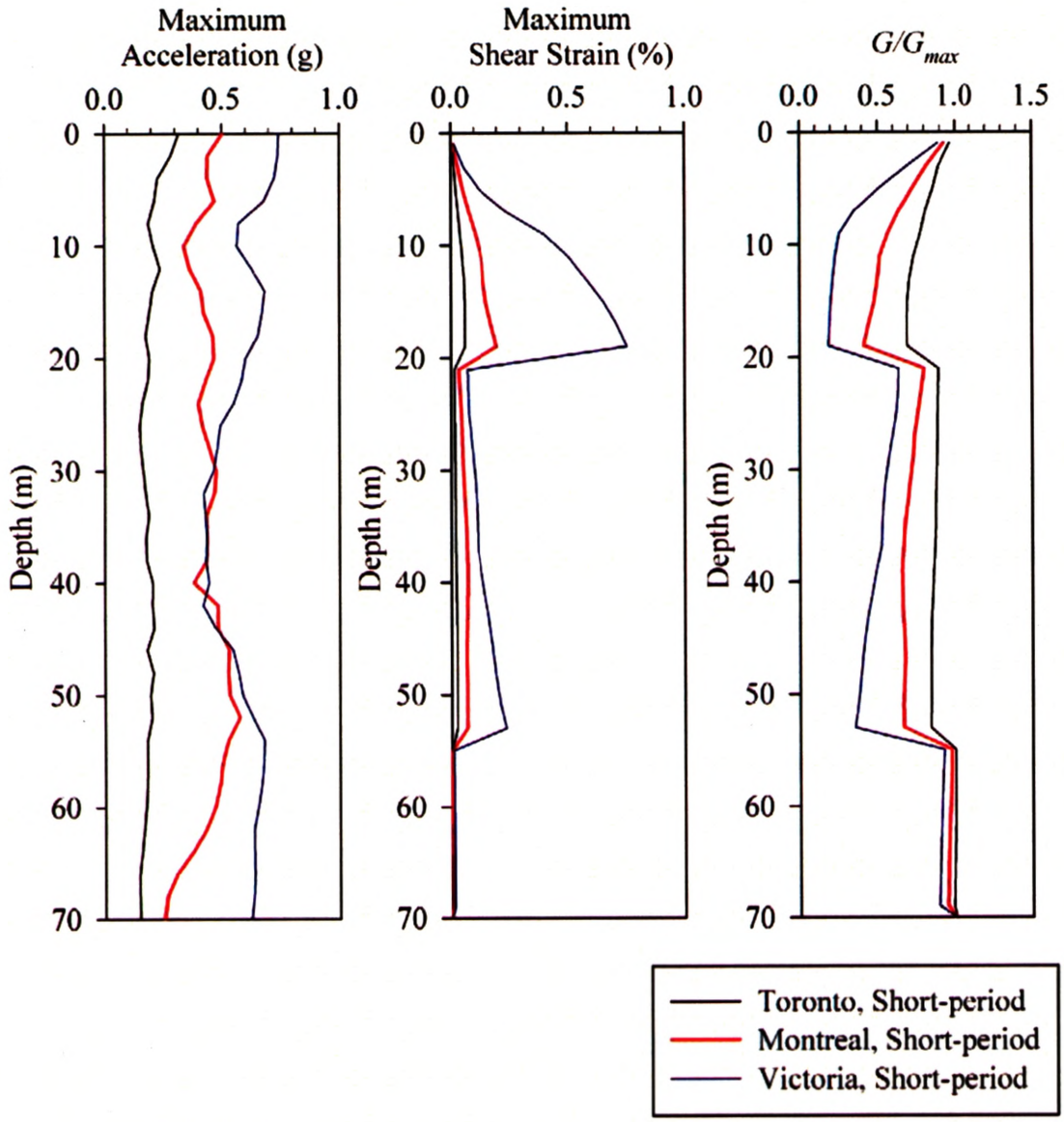

Figure 4.11: Maximum acceleration, shear strain and G/G_{max} predicted at BRCO by EERA.

G and V_s are related as shown Equation 4.4:

$$V_s = \sqrt{\frac{G}{\rho}} \tag{4.4}$$

where ρ is soil density. Thus, the reduction in V_s results in a shift of f_0 to a lower frequency.

It is also observed from the response spectra that, generally, the values of amplification predicted at each fundamental frequency decreased as the earthquake intensity increased. This reduction is the result of increased energy dissipation caused by strong motion relative to weak motion (Beresnev and Wen 1996).

4.3.4.1 Comparison with Empirical Spectra

While the numerical modelling techniques described previously are typically favoured by geotechnical engineers, seismologists tend to employ empirical techniques, such as the horizontal-to-vertical spectra ratio (HVSR) method of Lermo and Chavez-Garcia (1993). Figure 4.12 presents the theoretical spectra produced using the three programs for the Toronto earthquake, as well as empirical spectra calculated using the HVSR method. At all sites, empirical and theoretical predictions of f_0 are in reasonable agreement, while the empirical methods predict high values of amplification at this frequency. The HVSR method represents a linear method of analysis, particularly at the levels of shaking induced by earthquakes in this region. As a result, the empirical method predicts higher levels of amplification than the equivalent-linear and nonlinear methods.

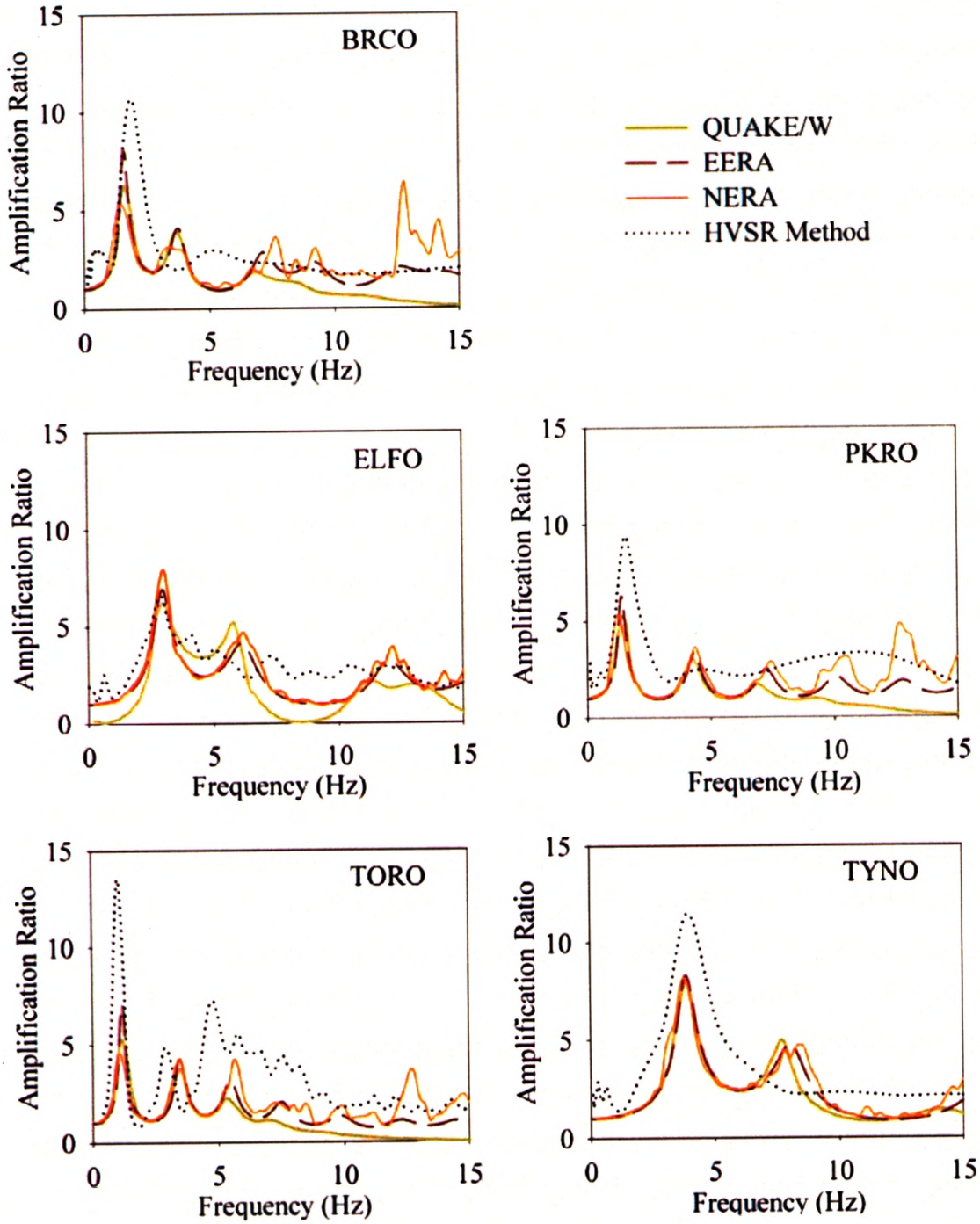

Figure 4.12: Comparison of empirical and theoretical spectra.

4.4 CONCLUSIONS

An investigation of the ground response modelling capabilities of three numerical programs, EERA, NERA and QUAKE/W, has been conducted. Using these programs, theoretical spectra were produced for five POLARIS-station sites for earthquakes of different intensities.

For low to moderate intensity earthquakes (Toronto, Montreal), the results from the three programs compare well with one another in terms of the predicted fundamental frequency (f_0) and corresponding amplitude.

For high intensity earthquakes (Victoria), however, the equivalent-linear programs, namely EERA and QUAKE/W, deviate from the nonlinear program NERA, indicative of the limitations of equivalent-linear approach for modelling site-response at high strain levels.

In all cases, QUAKE/W tends to underpredict response amplifications at higher frequencies, relative to EERA and NERA.

When compared with empirical spectra, numerical values predicted lower amplification at the fundamental frequency due to their simulating of nonlinear soil behaviour.

REFERENCES

Atkinson, G. (1999). "Ground motion time histories compatible with 2% in 50 years Uniform Hazard Spectra." <http://www.caee.uottawa.ca/Atkinson.pdf> (Dec. 1, 2007).

Atkinson, G. M. and Somerville, P. G. (1994). "Calibration of time history simulation methods." *Bulletin of the Seismological Society of America*, 84(2), 400-414.

Bardet, J. P., Iichi, K., and Lin, C. H. (2000). *EERA: A Computer Program for Equivalent Linear Earthquake Site Response Analysis of Layered Soil Deposits*, University of Southern California, Department of Civil Engineering.

Bardet, J. P, and Tobita, T. (2001). *NERA: A Computer Program for Nonlinear Earthquake site Response Analyses of Layered Soil Deposits*, University of Southern California, Department of Civil Engineering.

Beresnev, I., and Atkinson, G. M. (1997). "Shear wave velocity survey of seismographic sites in eastern Canada: calibration of empirical regression method of estimating site-response." *Seismological Research Letters*, 68(6), 981-987.

Beresnev, I. and Wen, K. (1996). "Nonlinear soil response - A reality?" *Bulletin of the Seismological Society of America*, 86(6), 1964-1978.

Idriss, I.M. and Sun, J.I. (1992). "SHAKE91: a computer program for conducting equivalent linear seismic response analyses of horizontally layered soil deposits." *User's Guide*, University of California.

Iwan, W. D. (1967). "On a class of models for the yielding behavior of continuous and composite systems." *Journal of Applied Mechanics*, 34, 612-617.

Krahn, J. (2004). *Dynamic Modelling with QUAKE/W: An Engineering Methodology,* GEO-SLOPE International Ltd., Calgary.

Kramer, S.L. (1996). *Geotechnical Earthquake Engineering*, Prentice Hall, New Jersey.

Lermo, J. F. and Chavez-Garcia, F. J. (1993). "Site effect evaluation using spectral ratios with only one station." *Bulletin of the Seismological Society of America*, 83(5), 1574-1594.

Mroz, Z. (1967). "On the description of anisotropic workhardening." Journal of Mechanics and Physics of Solids, 15, 163-175.

Murphy, C. (2003). "Near-surface characterization and estimated site response at POLARIS seismograph stations in southern Ontario, Canada." MSc thesis, University of Western Ontario, London, Ontario, Canada.

NBCC (2005). *National Building Code of Canada 2005,* Institute for Research and Construction, National Research Council of Canada, Ottawa, Ontario.

NEHRP (1994). *1994 Recommended provisions for seismic regulations of new buildings: Part 1, provisions*, FEMA 222A, National Earthquake Hazard Reduction Program, Federal Emergency Management Agency, Washington, D.C.

Schnabel, P.B., Lysmer, J., and Seed, H.B. (1972). "SHAKE: A Computer Program for Earthquake Response Analysis of Horizontally Layered Sites," *Report No. UBC/EERC-72/12, Earthquake Engineering Research Center*, University of California, Berkeley.

Sun, J.I., Golesorkhi, R. and Seed, H.B. (1988). "Dynamic Moduli and Damping Ratios for Cohesive Soils." *Report No. UCB/EERC-88/15, Earthquake Engineering Research Center*, University of California, Berkeley.

APPENDIX A

Table A.1: Foundation factors, *F* (NBCC, 1995).

Category	Type and depth of soil measured from the foundation or pile cap level	*F*
1	Rock, dense and very dense coarse-grained soils, very stiff and hard fine-grained soils; compact coarse-grained soils and firm and stiff fine-grained soils from 0 to 15 m deep	1.0
2	Compact coarse-grained soils, firm and stiff fine-grained soils with a depth greater than 15 m; very loose and loose coarse-grained soils and very soft and soft fine-grained soils from 0 to 15 m deep	1.3
3	Very loose and loose coarse-grained soils with depth greater than 15 m	1.5
4	Very soft and soft fine-grained soils with depth greater than 15 m	2.0

APPENDIX B

Table B.1: Events recorded at POLARIS stations.

Date	Origin Time	Latitude (°)	Longitude (°)	Depth (km)	Magnitude (m_N)
2004/07/01	19:41:43	43.4885	-79.5013	18.0	2.2
2004/07/06	11:09:32	43.6196	-78.0515	18.0	2.1
2004/07/15	4:30:44	42.0294	-82.3651	18.0	2.2
2004/07/18	23:54:30	46.8134	-77.9757	18.0	2.0
2004/07/22	13:10:00	46.5000	-74.9100	15.0	3.1
2004/07/24	18:19:01	54.0360	-85.4523	18.0	2.2
2004/08/04	23:55:26	43.6775	-78.2391	4.0	3.8
2004/08/11	20:19:51	49.5989	-91.8710	5.0	2.2
2004/08/17	5:10:52	46.9989	-76.8814	18.0	2.9
2004/08/25	14:21:25	52.8188	-81.2213	18.0	2.5
2004/09/04	2:05:31	44.8916	-74.9201	4.0	3.1
2004/09/06	19:31:46	46.1795	-75.1135	18.0	2.1
2004/09/21	14:17:34	50.1496	-94.2040	5.0	2.3
2004/09/22	20:42:50	52.3052	-81.0694	18.0	2.8
2004/09/28	21:10:25	44.6260	-81.5219	18.0	2.1
2004/10/04	6:56:02	49.0953	-91.9315	5.0	2.6
2004/10/10	12:34:39	46.0633	-76.0273	18.0	2.0
2004/10/10	23:39:05	45.5656	-73.7035	18.0	2.0
2004/10/11	8:33:50	49.6216	-81.4685	18.0	2.3
2004/10/27	2:25:03	44.4260	-78.2078	5.0	2.0
2004/11/03	13:02:04	48.6601	-91.1615	5.0	2.0
2004/11/23	16:46:04	46.8024	-75.8616	18.0	2.2
2004/11/23	17:04:08	48.1385	-79.6847	14.0	2.7
2004/11/23	18:32:58	48.2513	-79.6122	18.0	2.1
2004/11/30	21:49:21	47.3236	-76.9218	18.0	2.3
2005/03/02	06:53:17	41.8029	-80.9855	5.0	2.2
2005/03/03	02:22:01	45.0555	-74.2028	18.0	3.5
2005/03/13	04:02:04	40.5303	-84.7139	18.0	2.5
2005/03/13	17:08:14	46.5434	-80.9822	1.0	3.6
2005/03/15	03:08:05	43.0073	-78.0998	5.0	2.0
2005/03/28	16:39:38	43.3320	-79.2845	5.0	3.1
2005/03/28	16:58:28	43.3240	-79.2867	5.0	2.8
2005/03/31	02:27:34	43.3737	-78.5434	5.0	2.0
2005/03/31	14:29:58	52.4437	-80.9804	18.0	2.7
2005/03/31	15:13:08	46.2765	-75.6429	18.0	3.4
2005/04/05	11:03:49	53.0783	-80.9092	18.0	2.0
2005/04/08	04:32:38	46.2765	-73.4580	18.0	3.3
2005/04/08	05:37:55	53.0783	-82.7325	18.0	2.1
2005/04/09	08:53:15	46.2696	-91.7561	5.0	2.2
2005/04/15	23:58:42	47.4473	-73.8700	18.0	2.5
2005/04/17	00:18:38	51.5224	-73.7814	18.0	2.5
2005/04/17	18:48:28	49.8212	-81.4510	18.0	2.1

Table B.1: Events recorded at Ontario stations (continued)

2005/04/20	21:36:09	41.6162	-80.4093	5.0	2.2
2005/04/24	04:00:35	51.9653	-83.9345	18.0	2.0
2005/04/30	20:33:00	48.6000	-80.9300	-	3.0
2005/05/07	14:36:09	53.3544	-82.1711	18.0	2.6
2005/05/10	15:30:12	53.9614	-83.0061	18.0	2.8
2005/05/12	07:58:05	50.0082	-85.7257	18.0	2.0
2005/05/13	19:48:00	45.8000	-81.6300	-	3.0
2005/05/14	22:23:45	46.3814	-75.2220	18.0	2.0
2005/05/15	08:40:39	43.7792	-79.1541	5.0	2.0
2005/05/23	11:04:32	46.1061	-74.6990	18.0	2.4
2005/05/25	13:55:34	43.8427	-78.4205	5.0	2.1
2005/05/25	19:22:13	46.2743	-75.6164	18.0	3.7
2005/05/28	14:17:19	52.2858	-80.6808	18.0	2.2
2005/05/31	13:49:04	44.9730	-74.0685	18.0	2.9
2005/06/01	00:56:54	48.7969	-80.2996	18.0	2.0
2005/06/02	07:16:32	52.5389	-80.3407	18.0	2.0
2005/06/06	02:21:02	47.3097	-73.0392	18.0	2.1
2005/06/09	19:50:10	46.1061	-81.0486	18.0	2.5
2005/06/11	07:40:23	43.8427	-81.3994	18.0	2.0
2005/06/12	22:24:01	46.2743	-73.4269	18.0	2.7
2005/06/14	04:43:37	52.2858	-76.4483	18.0	2.7
2005/06/16	13:34:04	44.9730	-76.3413	18.0	2.1
2005/06/22	01:06:31	48.7969	-74.8536	18.0	2.0
2005/06/23	18:16:21	52.5389	-75.0504	18.0	3.0
2005/06/23	18:32:08	47.3097	-75.0472	18.0	3.3

APPENDIX C

```
function NAKAMURA(stat);
%
% This program is used to generate site response functions using
Nakamura's (1989) method.
% 'stat' is the name of a station.

% Checks station name is valid.

if length(stat)~= 4;
  'Invalid station name'
  return
end


% 'pickfiles' is text file listing the '.pick' files created previously
using the function picktimes.m.

fid1 = fopen('pickfiles.txt','r');

if fid1 < 0;
   'Work directory does not contain pickfiles.txt'
   return
end


dt = 0.01;
df = 0.2;
f = [0:df:1/(2*dt)];
icount = 0;
srbuf = zeros(length(f),1);
[pickfile,count] = fscanf(fid1,'%s',1);


% Reads data from the pickfile.

while count == 1;
    t1 = NaN;
    t2 = NaN;
    nt1 = NaN;
    nt2 = NaN;
    fid2 = fopen(pickfile,'r');
    [stattest,count2] = fscanf(fid2,'%s',1);

    while count2 > 0;
      [dummy,count2] = fscanf(fid2,'%f',4);

      if stattest == stat;
         t1 = dummy(1);
         t2 = dummy(2);
         nt1 = dummy(3);
         nt2 = dummy(4);
      end
      [stattest,count2] = fscanf(fid2,'%s',1);
    end
    fclose(fid2);

% Gathers data from the related eventfile using function 'uworead'.
```

```
    if ~isnan(t1);
        icount = icount + 1;
        eventfile = strcat(pickfile(1:length(pickfile)-4),'uwo');
        [titles,headers,data] = uworead(eventfile);
        [m,n] = size(data);
        indx = [0,0,0];
        j = 1;

        for iseis = 1:n;
            if titles(iseis,2:5) == stat;
                indx(j) = iseis;
                comp(j) = titles(iseis,9);
                j = j + 1;
            end
        end

        nn1 = round(nt1/dt + 1);
        nn2 = round(nt2/dt + 1);
        ti = 20;

        for j = 1:3;
            if comp(j) == 'Z';
                nzdat = data(nn1:nn2,indx(j));
            end
            if comp(j) == 'E';
                nedat = data(nn1:nn2,indx(j));
            end
            if comp(j) == 'N';
                nndat = data(nn1:nn2,indx(j));

            end
        end

        cnzdat = nzdat(1:(ti/dt)+1);
        cnedat = nedat(1:(ti/dt)+1);
        cnndat = nndat(1:(ti/dt)+1);

% Cosine tapers data using the function 'taper'.

        tnzdat = taper(cnzdat,5);
        tnedat = taper(cnedat,5);
        tnndat = taper(cnndat,5);

% Transforms the data and combines the horizontal spectra.

        nzspec1 = fft(tnzdat);
        nespec1 = fft(tnedat);
        nnspec1 = fft(tnndat);
        nhspec1 = sqrt(nespec1.*nespec1 + nnspec1.*nnspec1);

        ndftmp = 1/(dt*(length(cnzdat)-1));

% Smooths the data.
```

```
        for i = 2:(length(f)-1);
            flow = f(i-1);
            fhigh = f(i+1);
            nlow = round(flow/ndftmp) + 1;
            nhigh = round(fhigh/ndftmp)+ 1;
            nhspec(i) = mean(abs(nhspec1(nlow:nhigh)));
            nzspec(i) = mean(abs(nzspec1(nlow:nhigh)));
        end

        flow = f(1);
        fhigh = f(2);
        nlow = round(flow/ndftmp) + 1;
        nhigh = round(fhigh/ndftmp)+ 1;
        nzspec(1) = mean(abs(nzspec1(nlow:nhigh)));
        nhspec(1) = mean(abs(nhspec1(nlow:nhigh)));
        flow = f(length(f)-1);
        fhigh = f(length(f));
        nlow = round(flow/ndftmp) + 1;
        nhigh = round(fhigh/ndftmp)+ 1;
        nzspec(length(f)) = mean(abs(nzspec1(nlow:nhigh)));
        nhspec(length(f)) = mean(abs(nhspec1(nlow:nhigh)));

% Calculates the H/V spectral ratio.

       if icount == 1;
            srbuf = (abs(nhspec)./abs(nzspec))';
        else
            srbuf(:,icount) = (abs(nhspec)./abs(nzspec))';
        end
    end
[pickfile,count] = fscanf(fid1,'%s',1);
end

fclose(fid1);
xlswrite('Raw Data',srbuf);
site_resp = zeros(length(f),1);
sr_std = zeros(length(f),1);

for j = 1:length(f);
  site_resp(j) = mean(srbuf(j,:));
  sr_std(j) = std(srbuf(j,:));
end

nev = icount
plus = (site_resp)+(sr_std);
minus = (site_resp)-(sr_std);
resp = (cat(2,f',site_resp,sr_std,plus,minus));
xlswrite('Response',resp);
```

```
function HVSR(stat);
%
% This program is used to generate site response functions using HVSR
method of Lermo and Chavez-Garcia (1993).
% 'stat' is the name of a station.

% Checks that the station name is valid.

if length(stat)~= 4;
  'Invalid station name'
  return
end

% 'pickfiles' is text file listing the '.pick' files created previously
using the function picktimes.m.

fid1 = fopen('pickfiles.txt','r');
if fid1 < 0;
   'Work directory does not contain pickfiles.txt'
   return
end

dt = 0.01;
df = 0.2;
f = [0:df:1/(2*dt)];
threshold = 2.0;
icount = 0;
srbuf = zeros(length(f),1);
[pickfile,count] = fscanf(fid1,'%s',1);

% Reads data from the pickfile.

while count == 1;
    t1 = NaN;
    t2 = NaN;
    nt1 = NaN;
    nt2 = NaN;
    fid2 = fopen(pickfile,'r');
    [stattest,count2] = fscanf(fid2,'%s',1);

    while count2 > 0;
      [dummy,count2] = fscanf(fid2,'%f',4);

      if stattest == stat;
         t1 = dummy(1);
         t2 = dummy(2);
         nt1 = dummy(3);
         nt2 = dummy(4);
      end
      [stattest,count2] = fscanf(fid2,'%s',1);
    end

    fclose(fid2);

% Gathers both noise and earthquake data from the related eventfile
using function 'uworead'.
```

```
 if (~isnan(t1) & (t1 > 0));
        icount = icount + 1;
        eventfile = strcat(pickfile(1:length(pickfile)-4),'uwo');
        [titles,headers,data] = uworead(eventfile);
        [m,n] = size(data);
        indx = [0,0,0];
        j = 1;
        for iseis = 1:n;
            if titles(iseis,2:5) == stat;
                indx(j) = iseis;
                comp(j) = titles(iseis,9);
                j = j + 1;
            end
        end
        n1 = round(t1/dt + 1);
        n2 = round(t2/dt + 1);
        nn1 = round(nt1/dt + 1);
        nn2 = round(nt2/dt + 1);

        for j = 1:3;
            if comp(j) == 'Z';
                zdat = data(n1:n2,indx(j));
                nzdat = data(nn1:nn2,indx(j));
            end
            if comp(j) == 'E';
                edat = data(n1:n2,indx(j));
                nedat = data(nn1:nn2,indx(j));
            end
            if comp(j) == 'N';
                ndat = data(n1:n2,indx(j));
                nndat = data(nn1:nn2,indx(j));
            end
        end

% Cosine tapers data using the function 'taper'.

        tzdat = taper(zdat,5);
        tedat = taper(edat,5);
        tndat = taper(ndat,5);

        tnzdat = taper(nzdat,5);
        tnedat = taper(nedat,5);
        tnndat = taper(nndat,5);

% Transforms the data and combines the horizontal spectra.

        zspec1 = fft(tzdat);
        espec1 = fft(tedat);
        nspec1 = fft(tndat);
        hspec1 = sqrt(espec1.*espec1 + nspec1.*nspec1);

        nzspec1 = fft(tnzdat);
        nespec1 = fft(tnedat);
        nnspec1 = fft(tnndat);
        nhspec1 = sqrt(nespec1.*nespec1 + nnspec1.*nnspec1);
```

```
        dftmp = 1/(dt*(length(zdat)-1));
        ndftmp = 1/(dt*(length(nzdat)-1));

% Smooths the data.

        for i = 2:(length(f)-1);
            flow = f(i-1);
            fhigh = f(i+1);
            low = round(flow/dftmp) + 1;
            high = round(fhigh/dftmp)+ 1;
            zspec(i) = mean(abs(zspec1(low:high)));
            hspec(i) = mean(abs(hspec1(low:high)));

            nlow = round(flow/ndftmp) + 1;
            nhigh = round(fhigh/ndftmp)+ 1;
            nzspec(i) = mean(abs(nzspec1(nlow:nhigh)));
            nhspec(i) = mean(abs(nhspec1(nlow:nhigh)));
        end

        flow = f(1);
        fhigh = f(2);
        low = round(flow/dftmp) + 1;
        high = round(fhigh/dftmp)+ 1;
        zspec(1) = mean(abs(zspec1(low:high)));
        hspec(1) = mean(abs(hspec1(low:high)));

        nlow = round(flow/ndftmp) + 1;
        nhigh = round(fhigh/ndftmp)+ 1;
        nzspec(1) = mean(abs(nzspec1(nlow:nhigh)));
        nhspec(1) = mean(abs(nhspec1(nlow:nhigh)));

        flow = f(length(f)-1);
        fhigh = f(length(f));
        low = round(flow/dftmp) + 1;
        high = round(fhigh/dftmp)+ 1;
        zspec(length(f)) = mean(abs(zspec1(low:high)));
        hspec(length(f)) = mean(abs(hspec1(low:high)));

        nlow = round(flow/ndftmp) + 1;
        nhigh = round(fhigh/ndftmp)+ 1;
        nzspec(length(f)) = mean(abs(nzspec1(nlow:nhigh)));
        nhspec(length(f)) = mean(abs(nhspec1(nlow:nhigh)));

% Calculates the H/V spectral ratio.  Rejects values below the
threshold SNR.

       if icount == 1;
            srbuf = (abs(hspec)./abs(zspec))';
            hSNR = (abs(hspec)./abs(nhspec))';
            vSNR = (abs(zspec)./abs(nzspec))';
            for j = 1:length(f);
                if (hSNR(j) < threshold  | vSNR(j) < threshold);
                    srbuf(j) = NaN;
                end
            end
```

```
        else
            srbuf(:,icount) = (abs(hspec)./abs(zspec))';
            hSNR(:,icount) = (abs(zspec)./abs(nzspec))';
            vSNR(:,icount) = (abs(zspec)./abs(nzspec))';
            for j = 1:length(f);
                if (hSNR(j,icount) < threshold | vSNR(j,icount) <
threshold);
                    srbuf(j,icount) = NaN;
                end
            end
        end
    end
[pickfile,count] = fscanf(fid1,'%s',1);
end

fclose(fid1);
xlswrite('Raw Data',srbuf);
site_resp = zeros(length(f),1);
sr_std = zeros(length(f),1);

for j = 1:length(f);
  site_resp(j) = nanmean(srbuf(j,:));
  sr_std(j) = nanstd(srbuf(j,:));
end

nev = icount
plus = (site_resp)+(sr_std);
minus = (site_resp)-(sr_std);
resp = (cat(2,f',site_resp,sr_std,plus,minus));
xlswrite('Response',resp);
```

APPENDIX D

Table D.1: Theoretical fundamental frequency (f_0) and peak amplification (A) values.

Site	Earthquake	EERA		QUAKE/W		NERA	
		f_0 (Hz)	A	f_0 (Hz)	A	f_0 (Hz)	A
BRCO	Toronto, Short-period	1.6	8.1	1.6	6.3	1.4	5.2
	Montreal, Short-period	1.4	7.0	1.4	5.8	1.2	3.5
	Montreal, Long-period	1.4	5.9	1.4	5.9	1.4	4.8
	Victoria, Short-period	1.0	5.0	1.0	4.3	1.2	1.5
	Victoria, Long-period	1.2	6.1	1.2	5.3	1.4	4.5
ELFO	Toronto, Short-period	2.8	5.9	3.0	6.9	3.0	7.9
	Montreal, Short-period	2.8	6.6	2.6	5.7	2.6	5.4
	Montreal, Long-period	2.6	6.2	2.6	6.2	2.6	4.9
	Victoria, Short-period	2.2	5.8	2.2	5.8	2.0	3.0
	Victoria, Long-period	2.2	6.1	2.2	5.3	2.4	5.5
PKRO	Toronto, Short-period	1.4	6.3	1.4	5.2	1.2	5.2
	Montreal, Short-period	1.2	4.7	1.2	4.7	1.2	3.1
	Montreal, Long-period	1.2	5.4	1.2	5.4	1.2	3.8
	Victoria, Short-period	0.8	3.3	0.8	3.3	1.2	1.3
	Victoria, Long-period	1.0	4.5	1.0	4.5	1.2	3.8
TORO	Toronto, Short-period	1.2	7.1	1.2	5.2	1.0	4.5
	Montreal, Short-period	1.0	5.4	1.0	4.4	1.0	3.6
	Montreal, Long-period	1.0	5.4	1.0	4.5	0.8	3.0
	Victoria, Short-period	0.6	3.9	0.4	2.6	0.6	1.1
	Victoria, Long-period	0.8	3.5	0.6	4.4	0.6	4.4
TYNO	Toronto, Short-period	3.8	7.9	3.8	7.9	3.8	7.9
	Montreal, Short-period	3.6	7.2	3.4	6.7	3.2	5.0
	Montreal, Long-period	3.2	7.2	3.2	7.2	3.5	5.1
	Victoria, Short-period	2.2	8.5	2.6	5.7	2.2	3.8
	Victoria, Long-period	2.4	5.9	2.8	6.6	3.8	7.3